Chapter 1

INTRODUCTION

1.1 Introduction

Pyrrhotite $Fe_{(1-x)}S$ is one of the most commonly occurring metal sulfide minerals and is recognised in a variety of ore deposits including nickel-copper, lead-zinc, and platinum group element (PGE). Since the principal nickel ore mineral, pentlandite, almost ubiquitously occurs coexisting with pyrrhotite, the understanding of the behaviour of pyrrhotite during flotation is of fundamental interest. For many nickel processing operations, pyrrhotite is rejected to the tailings in order to control circuit throughput and concentrate grade and thereby reduce excess sulfur dioxide smelter emissions (e.g. Sudbury; Wells *et al.*, 1997). However, for platinum group element processing operations, pyrrhotite recovery is targeted due to its association with the platinum group elements and minerals (e.g. Merensky Reef; Penberthy and Merkle, 1999; Ballhaus and Sylvester, 2000). Therefore, the ability to be able to manipulate pyrrhotite performance in flotation is of great importance. It can be best achieved if the mineralogical characteristics of the pyrrhotite being processed can be measured and the relationship between mineralogy and flotation performance is understood.

The pyrrhotite mineral group is non-stoichiometric and has the generic formula of $Fe_{(1-x)}S$ where $0 \leq x < 0.125$. Pyrrhotite is based on the nickeline (NiAs) structure and is comprised of several superstructures owing to the presence and ordering of vacancies within its structure. Numerous pyrrhotite superstructures have been recognised in the literature, but only three of them are naturally occurring at ambient conditions (Posfai *et al.*, 2000; Fleet, 2006). This includes the stoichiometric FeS known as troilite which is generally found in extraterrestrial localities, but on occasion, has also been recognised in some nickel deposits (e.g. Voisey's Bay, Bushveld Igneous Complex; Liebenberg, 1970; Naldrett *et al.*, 2000). The commonly occurring magnetic pyrrhotite is correctly known as 4C pyrrhotite, has an ideal composition Fe_7S_8 and monoclinic crystallography (Powell *et al.*, 2004). Non-magnetic pyrrhotite is formally described as *N*C pyrrhotite where *N* is an integer between 5 and 11 (Morimoto *et al.*,

1970). Non-magnetic NC pyrrhotite has a range of ideal compositions varying from Fe_9S_{10}, $Fe_{10}S_{11}$ to the least iron deficient composition of $Fe_{11}S_{12}$. Although NC pyrrhotite is generally known as "hexagonal pyrrhotite", it has been argued to be pseudohexagonal and may actually be monoclinic or orthorhombic (Carpenter and Desborough, 1964; Morimoto *et al.*, 1970; Koto *et al.*, 1975; Posfai *et al.*, 2000).

Pyrrhotite is known to be a reactive mineral which is highly prone to oxidation (Rand, 1977; Belzile *et al.*, 2004). The downstream consequences of this during minerals beneficiation may be quite severe, an example of which is the Nickel Rim site in Sudbury described by Johnson *et al.* (2000). The Nickel Rim site is actively suffering from the release of low pH waters, high concentrations of iron, and dissolved metals such as nickel and aluminium and will likely suffer from this continual discharge for at least another half century. Pyrrhotite from the Sudbury ore deposit was acknowledged as the source of the acid mine drainage (AMD). However, in terms of flotation, the reactivity of pyrrhotite towards excessive oxidation may have a detrimental effect on its flotation performance due to the formation of hydrophilic iron hydroxides that render surfaces of pyrrhotite particles less floatable. Therefore, the influence of pyrrhotite mineralogy upon oxidation and oxidation rates is also of interest.

Accounts in the literature are somewhat contradictory, but more frequently attribute monoclinic pyrrhotite to be the more reactive phase (e.g. Vanyukov and Razumovskaya, 1979; Yakhontova *et al.,* 1983; both in Russian and quoted by Janzen, 1996). More recently, using ToF-SIMS, Gerson and Jasieniak (2008) similarly showed that the oxidation rate of monoclinic pyrrhotite was greater than "hexagonal" pyrrhotite. Orlova *et al.* (1988) however (in Russian, quoted by Janzen, 1996), suggested that "hexagonal" pyrrhotite was more reactive. Janzen (1996) showed no correlation between pyrrhotite crystal structure and oxidation rate. Kwong (1993) suggested that the oxidation rate of pyrrhotite enriched in trace metals was slower than those with low nickel and cobalt contents. In the leaching study of Lehmann *et al.* (2000) it was shown that "hexagonal" pyrrhotite from two Australian locations was less susceptible to cyanide leaching than monoclinic pyrrhotite.

Accounts in the literature with respect to the flotation behaviour of magnetic and non-magnetic pyrrhotite are similarly quite varied. According to Iwasaki (1988), it was noted by Harada (1967; In Japanese) that samples of freshly ground monoclinic pyrrhotite were more floatable than "hexagonal" pyrrhotite although the reverse occurred on more oxidised

samples. Kalahdoozan (1996) showed that synthetic "hexagonal" pyrrhotite exhibited better xanthate adsorption and flotation recovery at a higher pH (≥ 10), whereas at a lower pH (7 - 8.5) monoclinic pyrrhotite was more floatable. Using pyrrhotite samples derived from the Mengzi lead zinc ore deposit, M.F. He *et al.* (2008) also showed that monoclinic pyrrhotite was more floatable than "hexagonal" pyrrhotite. Others such as Lawson *et al.* (2005) and Wiese *et al.* (2005) have demonstrated that differences in flotation performance between different pyrrhotite types exist. Lawson *et al.* (2005) showed a difference in pyrrhotite recovery between non-magnetic and magnetic circuits of the Sudbury ore where pyrrhotite depression was targeted. Similarly, results of batch flotation tests performed on Bushveld Merensky Reef ores by Wiese *et al.* (2005) have shown that the recovery of pyrrhotite from Merensky Reef ore from one location was greatly increased when copper sulfate was used as an activator during flotation, whereas for ore from another location the effect of copper sulfate addition on pyrrhotite recovery was minor. It is probable that these differences in recovery may have been due to the differences in pyrrhotite mineralogy.

Various process mineralogy studies on a range of operations have shown the benefit achieved by concentrators when a complete characterisation of the ore was undertaken in conjunction with experimental tests to determine its metallurgical performance (Bojecevski *et al.*, 1998; Baum *et al.*, 2006; Charland *et al.*, 2006; Brough, 2008). This suggests that in order to be able to successfully optimise or control the behaviour of an ore during flotation, a comprehensive understanding of its mineralogy and relationship to flotation behaviour is needed. It is probable that the lack of agreement in studies comparing pyrrhotite flotation and oxidation to crystallography and trace metal content may be due to the fact that only limited aspects of the pyrrhotite mineralogy were examined.

1.2 Aim of this Study

The aim of this process mineralogy study was to develop the relationship between pyrrhotite mineralogy and flotation performance based on a thorough characterisation of pyrrhotite from selected nickel and platinum group element ore deposits in terms of its crystallography, mineral association, mineral chemistry and mineral reactivity. By linking key characteristics of pyrrhotite mineralogy and reactivity to variations in the flotation performance through carefully controlled microflotation experiments of magnetic, non-magnetic and mixed pyrrhotite, an understanding of the reasons and mechanisms behind these differences in pyrrhotite flotation performance was sought. An additional goal of importance was to show which mineralogical measurements have shown the most potential in developing the relationship between pyrrhotite mineralogy and flotation performance.

1.3 Key Questions

The objectives of this work were met by addressing the following key questions:

(i) How does the mineral association, mineral chemistry and crystallography vary between magnetic and non-magnetic pyrrhotite?

(ii) How does ore deposit formation affect the mineralogy of pyrrhotite?

(iii) How does the reactivity of magnetic and non-magnetic pyrrhotite differ? Can these differences be accounted for in terms of the:
a) crystallography
b) mineral chemistry
c) mineral association of pyrrhotite?

(iv) How does the flotation performance of magnetic and non-magnetic pyrrhotite differ? Can these differences be accounted for in terms of the:
a) crystallography
b) mineral chemistry
c) mineral association of pyrrhotite?

1.4 Scope of Research

Since the fields of ore geology and mineral processing are extremely diverse, the scope and boundaries of this process mineralogy study are illustrated by figure 1.1. The only mineralogical components of ore geology that are relevant, are the petrography, mineral chemistry and crystallography of pyrrhotite from selected nickel and platinum group element ore deposits. Pyrrhotite crystallography is only investigated in terms of the unit cell dimensions in order to determine pyrrhotite superstructures and does not extend to any molecular modelling of the stability of the pyrrhotite crystal structure. The focus of this study is on pyrrhotite mineralogy and therefore excludes additional silicate and oxide minerals.

Mineral reactivity, which is considered to be a consequence of the interaction of pyrrhotite with the environment, is considered, but only selected measurements are investigated in order to determine differences in the reactivity of magnetic and non-magnetic pyrrhotite towards oxidation. These measurements include the use of open circuit potential, cyclic voltammetry and oxygen uptake. Specialised techniques such as XPS and ToF-SIMS also provide detailed information on the reactivity of mineral surfaces and with the addition of EDTA are considered as potential areas for further research focus (see recommendations in Chapter 8). Although some previous studies have compared the reactivity of different pyrrhotite types using flow through reactor experiments in order to determine oxidation rate constants (e.g. Janzen, 1996), reactivity measurements in this study are used as a characterisation method in order to develop the relationship between mineralogy and flotation performance.

Within the field of mineral processing, the separation process of flotation is the primary focus in this study. Pyrrhotite flotation performance is measured using carefully controlled microflotation experiments. Therefore, aspects relating to the breakage such as the comminution method, particle size distribution and liberation characteristics of both valuable and gangue minerals will not be focussed upon. However, the liberation of pyrrhotite will be of interest in terms of its mineral association to pentlandite. Other aspects of flotation such as the presence of a froth phase, pulp rheology, circuit performance and flotation scale up also fall beyond the scope of this study.

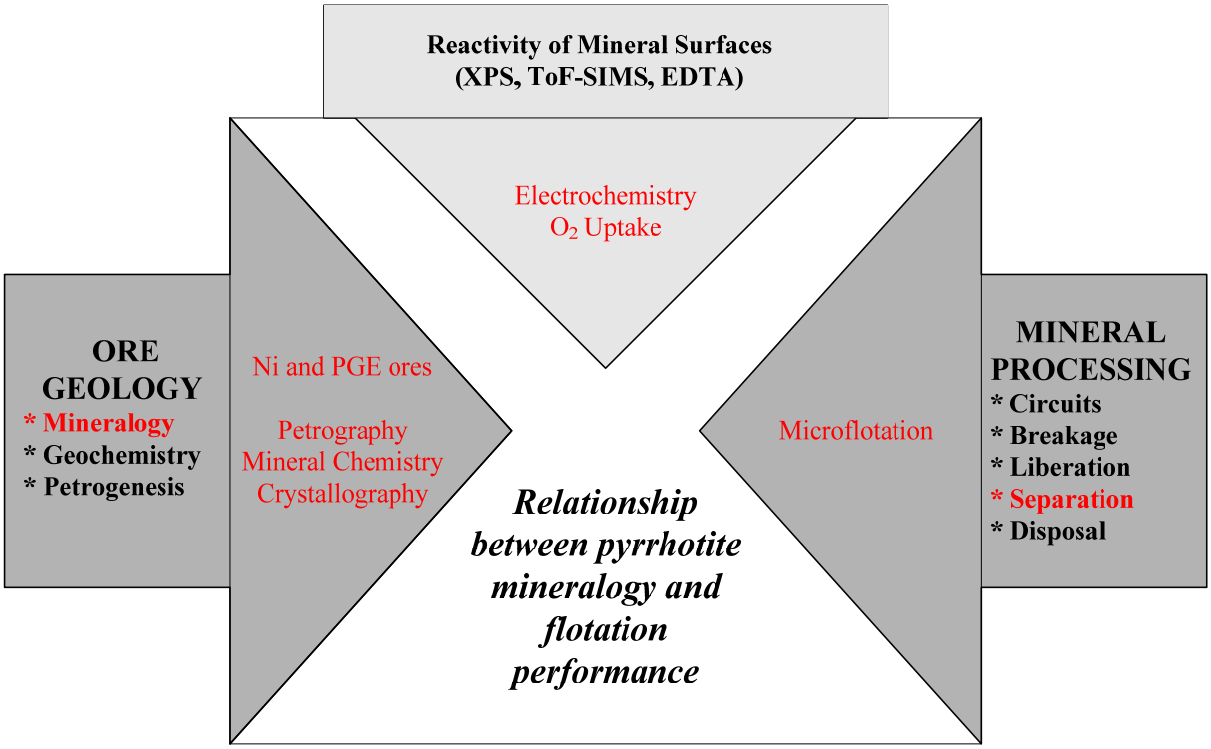

Figure 1.1: Schematic of the scope of research in this study with key areas of interest highlighted in red.

1.5 Organisation of the Thesis

The body of this thesis is divided into eight chapters starting with the Introduction where the background, scope of the thesis and key questions are presented in Chapter 1. This is followed by a critical review of the literature in Chapter 2 on pyrrhotite ore deposits, pyrrhotite mineralogy, the electrochemical properties of pyrrhotite, pyrrhotite flotation and the field of process mineralogy. Chapter 3 describes sampling and analytical methods. The results are then divided into three chapters; Chapter 4 describes the mineralogical characterisation of the pyrrhotite samples, Chapter 5 describes the reactivity of the pyrrhotite samples and Chapter 6 describes the flotation of the pyrrhotite samples. A discussion and linkage of these results in order to determine the effect of pyrrhotite mineralogy on flotation performance is given in Chapter 7. Some final conclusions as well as several recommendations for further research are given in Chapter 8. The complete set of results from the various experiments is given in the Appendices.

Chapter 2

LITERATURE REVIEW

2.1 Overview of Pyrrhotite Ore Deposits

Pyrrhotite is one of the most commonly occurring sulfide minerals, with associations to nickel deposits, platinum group element deposits, as well as copper lead zinc type deposits. Geologically, nickel ore deposits are classified according to their mode of occurrence and petrogenesis and are broadly classified into those related to magmatic events and the laterite deposits. The laterite deposits are generally found in equatorial or paleoequatorial locations. Magmatic sulfide deposits can be described as those nickel copper and platinum group element sulfide deposits which have formed through the interaction of mantle material with continental crust. Following the classification scheme of Naldrett (1989) they can be further subdivided into groups according to their association with:

i). Synvolcanic deposits often associated with greenstone belts e.g. Kambalda, W. Australia.
ii). Rifted plate margins and ocean basins e.g. Thompson Belt, Manitoba, Canada.
iii). Intrusions in cratonic areas e.g. Noril'sk Talnakh, Russia; Bushveld Igneous Complex, South Africa and the Sudbury Igneous Complex, Canada.
iv). Intrusions in orogenic belts: e.g. Aberdeenshire, Scotland.

The literature reviewed here, is focused on pyrrhotite occurrences selected for this study. These are related to the stratiform deposits occurring as intrusions in cratonic areas (Bushveld Igneous Complex, Sudbury Igneous Complex) and as those in association with Archean greenstone belts (Tati greenstone belt).

2.1.1 Bushveld Igneous Complex, South Africa

The Bushveld Igneous Complex in South Africa is one of the worlds largest economic platinum group element resources with estimates of 204 and 116 million ounces of proven reserves for platinum and palladium, respectively (Cawthorn, 1999). The layered complex has an aerial extent on the order of 65 000 km^2 and is thought to extend into Botswana to the Molopo Farms Complex (Eales and Cawthorn, 1996). The Proterozoic Bushveld Complex is comprised of various limbs, shown in figure 2.1, that formed during the Bushveld Super-Event. The economic horizon of the Complex is known as the Rustenburg Layered Suite (SACS, 1980), a transitional layered series representing the influx of multiple injections of magma into the continental crust. Within the Critical Zone of the Rustenburg Layered Suite occurs the Upper Group Chromitite (UG2) Reef, which is stratigraphically overlain by the Merensky Reef as illustrated by the stratigraphic column in figure 2.2. Both reefs are exploited for their PGE content, although the base metal sulfides (BMS) are recovered as a by product from the Merensky Reef. A third reef type known as Platreef is also exploited for PGEs. The Platreef is restricted to the Northern limb of the Complex, whereas the Merensky Reef and UG2 Reef are present in both the Eastern and Western limbs.

Pyrrhotite samples for characterisation in this study are derived from the Merensky Reef named after Dr Hans Merensky, who first discovered the in-situ location and recognised the importance of this platinum group element bearing ore body in 1924 (Cawthorn, 1999). The terminology “Merensky Reef” is generally used to represent the economic mining cut situated within the basal section of the “Merensky Cyclic Unit”. It should be noted that any description of the Merensky Reef will not adequately capture the variation in lithology and texture of the reef along strike due to its heterogenous character (Farquhar, 1986; Leeb-Du Toit, 1986; Viljoen and Hieber, 1986; Viljoen *et al.*, 1986; Viring and Cowell, 1999). The footwall of the Merensky cyclic unit is comprised of a norite to anorthosite with a sharp contact to the overlying thin basal chromitite layer (~1 cm thick). Sandwiched between the basal chromitite and an upper chromitite layer (known as the Merensky chromitite) is a feldspathic pegmatoidal pyroxenite. The thickness of this pegmatoidal layer varies quite considerably from mine to mine. In some locations on the Western limb, this pegmatoidal layer is absent (e.g. Impala platinum mines; Leeb-Du Toit, 1986) whereas towards the northern most mines of the Western limb (e.g. Northam Platinum Mine; Viring and Cowell, 1999) this pegmatoidal pyroxenite layer may be up to several metres thick. The Merensky

chromitite is typically a few centimetres in thickness. Overlying the Merensky chromitite, is a pyroxenite which gradually changes into norite and even anorthosite (Farquhar, 1986; Leeb-Du Toit, 1986; Viljoen and Hieber, 1986; Viljoen *et al.*, 1986; Viring and Cowell, 1999).

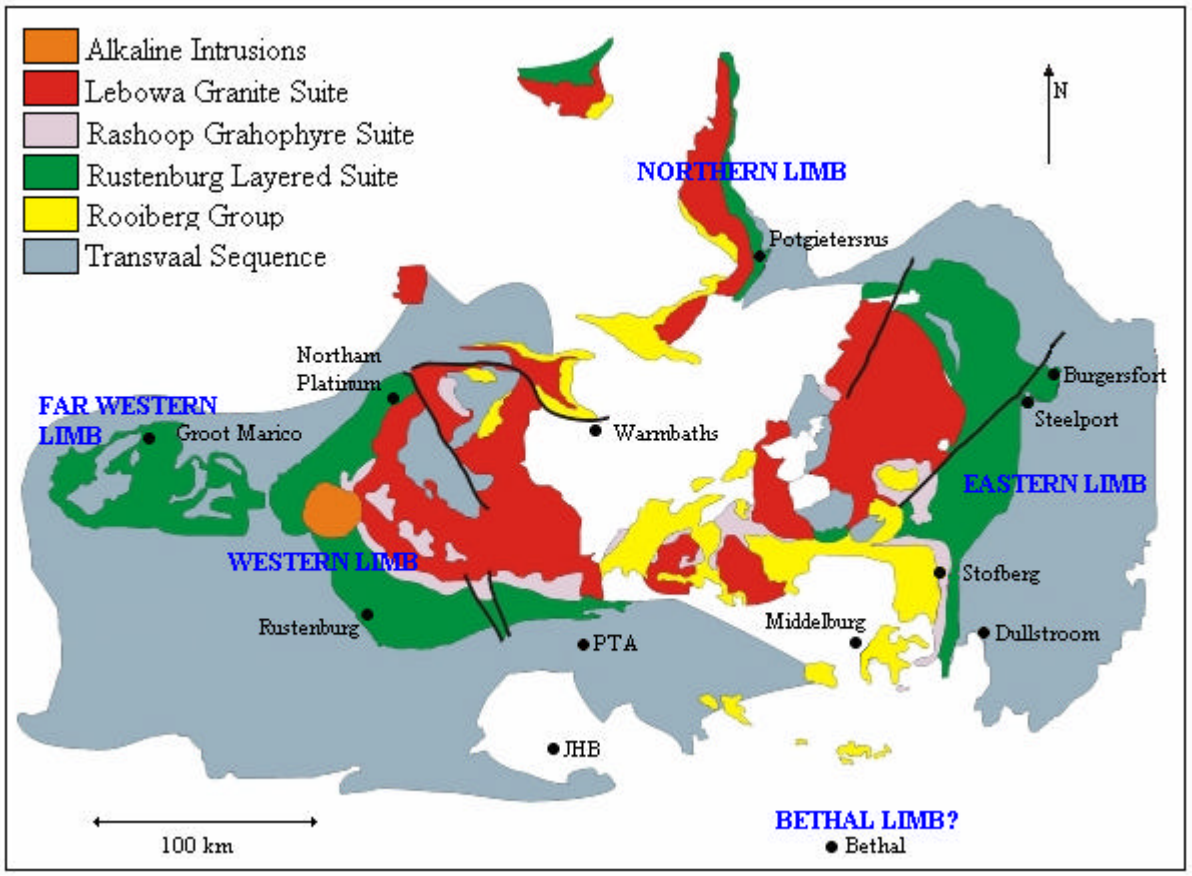

Figure 2.1: Map of the Bushveld Igneous Complex, illustrating the location of the Rustenburg Layered Suite, host to the Merensky Reef, in the Bushveld Igneous Complex. From: Brough (2008).

Base metal sulfides and associated platinum group minerals are typically interstitial to the coarse grained pyroxene and plagioclase and are enriched within the vicinity of the Merensky chromitite. The sulfides generally constitute a few weight percent of the Merensky Reef. The observed sulfides are pyrrhotite, pentlandite, chalcopyrite and pyrite in decreasing order of abundance and typically occur as multi-mineralic granular aggregates. Lesser cubanite, mackinawite, sphalerite, bornite, vallerite and troilite have also been recognised (Liebenberg, 1970). Platinum group mineralization at 5-7 g/t (Cawthorn *et al.*, 2002) occurs as either discrete platinum group minerals such as sulfides, tellurides, arsenides and alloys or in solid solution with the sulfides (Kinloch, 1982; Schouwstra *et al.*, 2000; Cabri *et al.*, 2008). In the study of Ballhaus and Sylvester (2000), concentrations of the platinum group elements

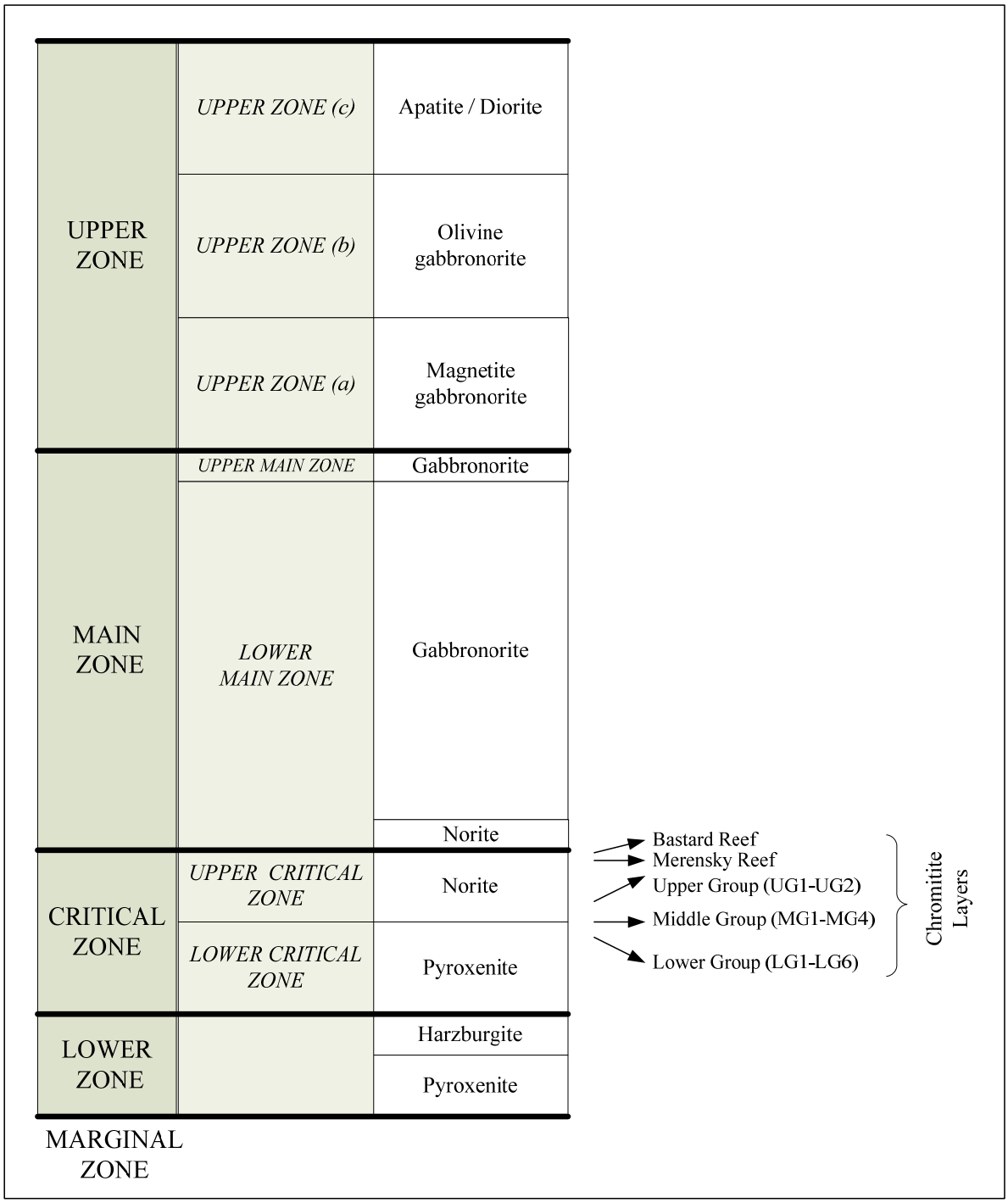

Figure 2.2: Generalised stratigraphy of the Rustenburg Layered Suite, of the Bushveld Igneous Complex. The stratigraphic position of the Merensky Reef is also shown. Adapted from Eales and Cawthorn (1996).

were detected in both pyrrhotite and pentlandite. Osmium, iridium and ruthenium in particular, were detected in solid solution with pyrrhotite.

2.1.2 Uitkomst Complex, South Africa

The Uitkomst Complex in South Africa is situated in the Mpumalanga Province near Badplaas. Mining of the economic mineralisation in the Uitkomst Complex takes places at the Nkomati Nickel Mine. The Uitkomst Complex is situated just east of the Eastern Limb of the Bushveld Complex as shown in figure 2.3a. Since it is similar in age and character to the Bushveld Igneous Complex, it has been argued to be related to the Bushveld Igneous Complex (Gauert *et al.*, 1995; Gauert, 2001). As illustrated by figure 2.3b and c, the Uitkomst Complex is an elongate intrusion that consists of a series of defined lithological units of gabbros, harzburgites, gabbronorites and pyroxenites that form a trough-like shape 750 m in thickness and between 650 and 1600 m in width (Gauert, 2001). A series of mineralised zones exist and which are summarised in table 2.1. In the past, mining was concentrated within the massive sulfide body (MSB) located beneath the Basal Gabbro in the Uitkomst Complex. Currently mining is focused on exploiting the more disseminated ores located in the Main Mineralised Zone (MMZ) and the Chromititic Peridotite Mineralised Zones.

Sulfide mineralization in the Uitkomst Complex occurs in a variety of textural types that includes disseminated sulfides, net-textured sulfides, local concentrations of sulfides and as massive sulfide ore (Gauert *et al.*, 1995; van Zyl, 1996). The most common sulfide minerals are pyrrhotite, pentlandite, chalcopyrite and pyrite in decreasing order of abundance. Minor sulfide minerals present are digenite, mackinawite, galena, sphalerite, millerite and arsenopyrite. The oxide minerals, magnetite, ilmenite and chromite are common. Enrichment of the PGE also occurs as discrete platinum-palladium tellurides (merenskyite, michenerite, testibiopalladite) or as the arsenides (sperrylite). Unlike the platinum group mineralisation in the Merensky Reef, platinum-palladium sulfide minerals are not common (Theart and de Nooy, 2001).

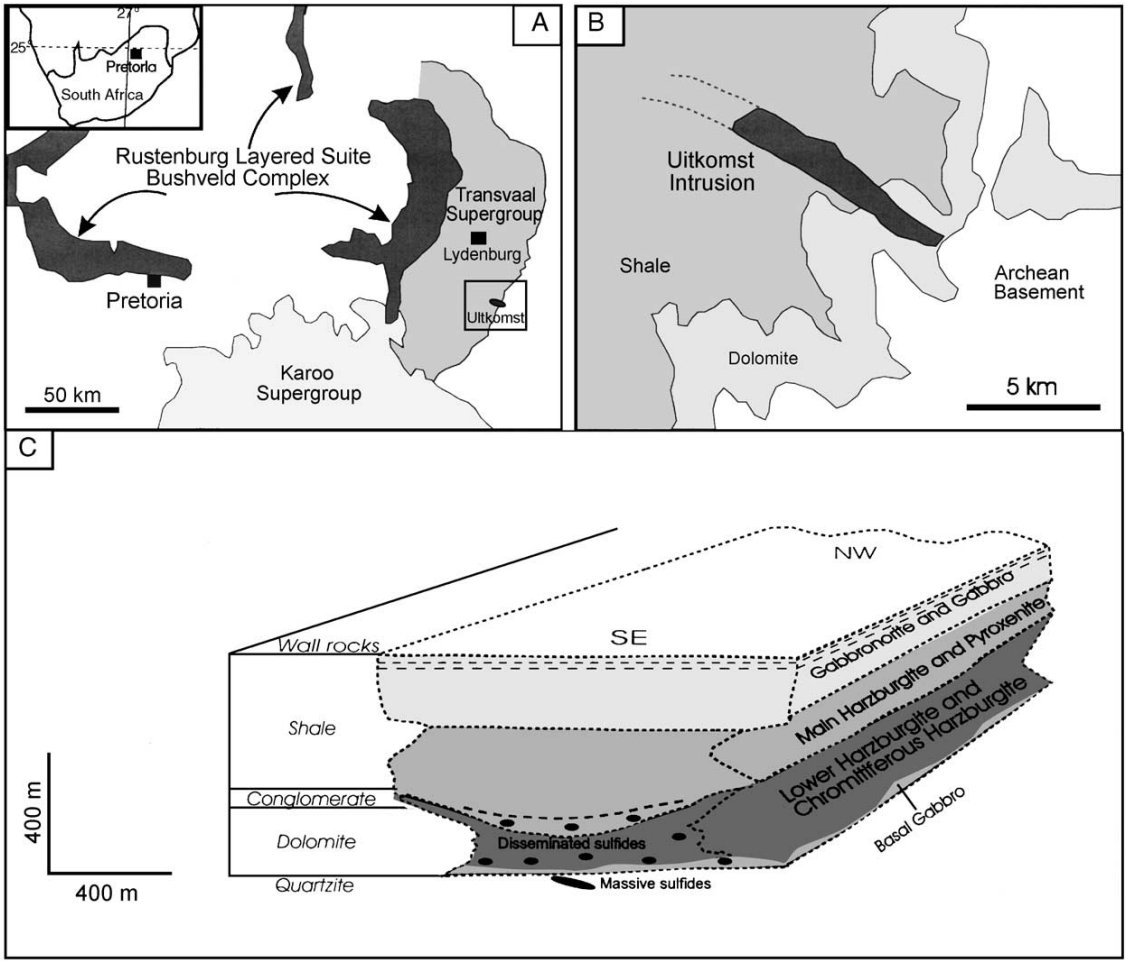

Figure 2.3: (a) Location of the Uitkmost Complex in relation to the Bushveld Complex in South Africa. (b) Strike of the Uitkomst intrusion and (c) Cross section of the Uitkomst intrusion showing the location of massive and disseminated sulfides. From: Li *et al.* (2002).

Table 2.1: Stratigraphy of the Uitkomst Complex with associated sulfide mineralisation. Adapted from: Theart and de Nooy (2001).

Group	Unit	Thickness (m)	Mineralisation
Main	Gabbronorite	262	-
	Upper Pyroxenite	66	-
	Peridotite/Harzburgite	264	-
	Massive Chromitite	(0-6)	-
Basal	Chromititic Peridotite	35	Chromititic Peridotite Mineralised Zone (PCMZ)
	Lower Pyroxenite	37	Main Mineralised Zone (MMZ)
	Basal Gabbro	35	Basal Mineralised Zone (BMZ)
(Basement)	Massive Sulfide Body (MSB)	26	Upper Stringer Zone Massive Stringer Zone Lower Stringer Zone

2.1.3 Phoenix Deposit, Botswana

The Phoenix ore deposit forms part of the Archean Tati greenstone belt situated near Francistown in Botswana as shown in figure 2.4a. In addition to the Phoenix sulfide deposit, the Selkirk and Tekwane sulfide deposits have been recognised (Figure 2.4b). The greenstone belt has been subjected to lower greenschist and lower amphibolite facies metamorphism and comprises a series of meta-volcanics, meta-sedimentary rocks and granitoids. The Phoenix ore body is hosted by meta-gabbronorite, whereas the Selkirk and Tekwane ore bodies are hosted by a granular meta-gabbro (Johnson, 1986; Maier *et al.*, 2008). Mineralisation at Phoenix occurs as a series of elongate north-south and east-west trending lenses of massive sulfide ore. These lenses are typically only 1.5 m in diameter although are tens of metres in length (Johnson, 1986; Maier *et al.*, 2008). Sulfide minerals present include pyrrhotite, pentlandite and chalcopyrite with lesser sphalerite, molybdenite and galena. The Selkirk and Tekwane deposits are similar in mineralogy to Phoenix, except that they are characterised by the presence of magnetite and pyrite.

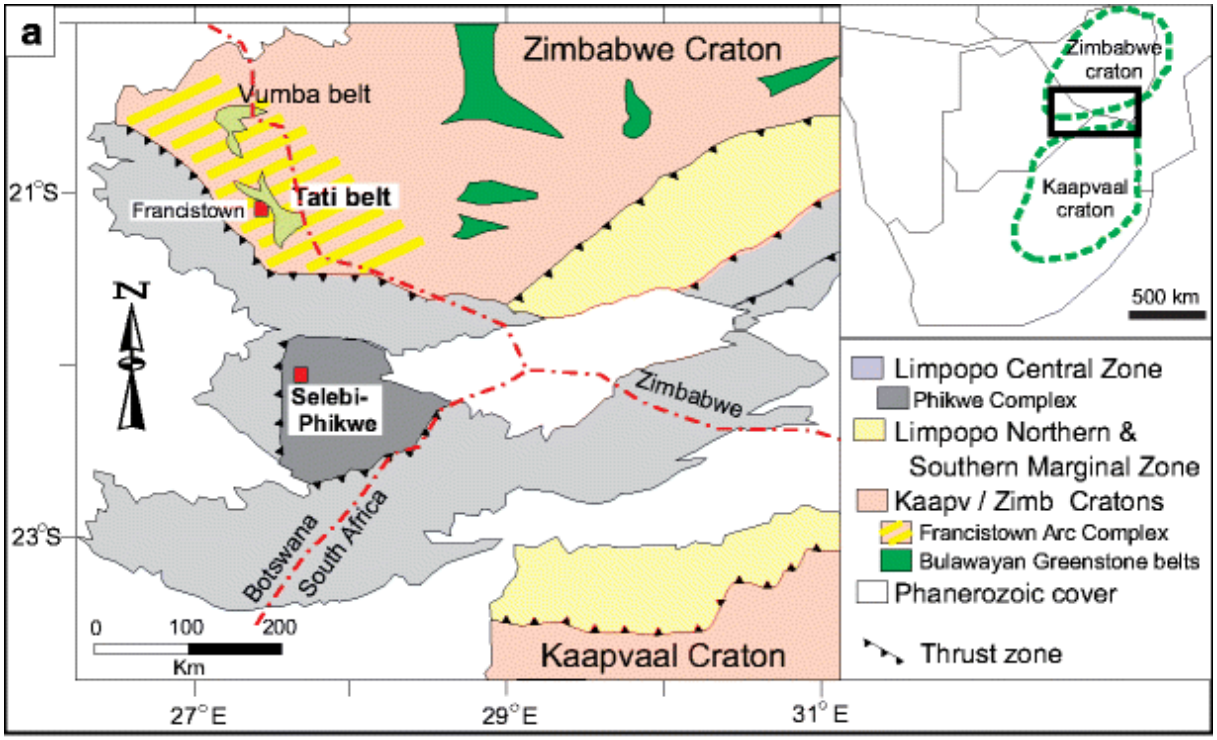

Figure 2.4: (a) Location of the Tati greenstone belt in Botswana. (b) Location of the Phoenix, Selkirk and Tekwane ore deposits. From: Maier *et al.* (2008).

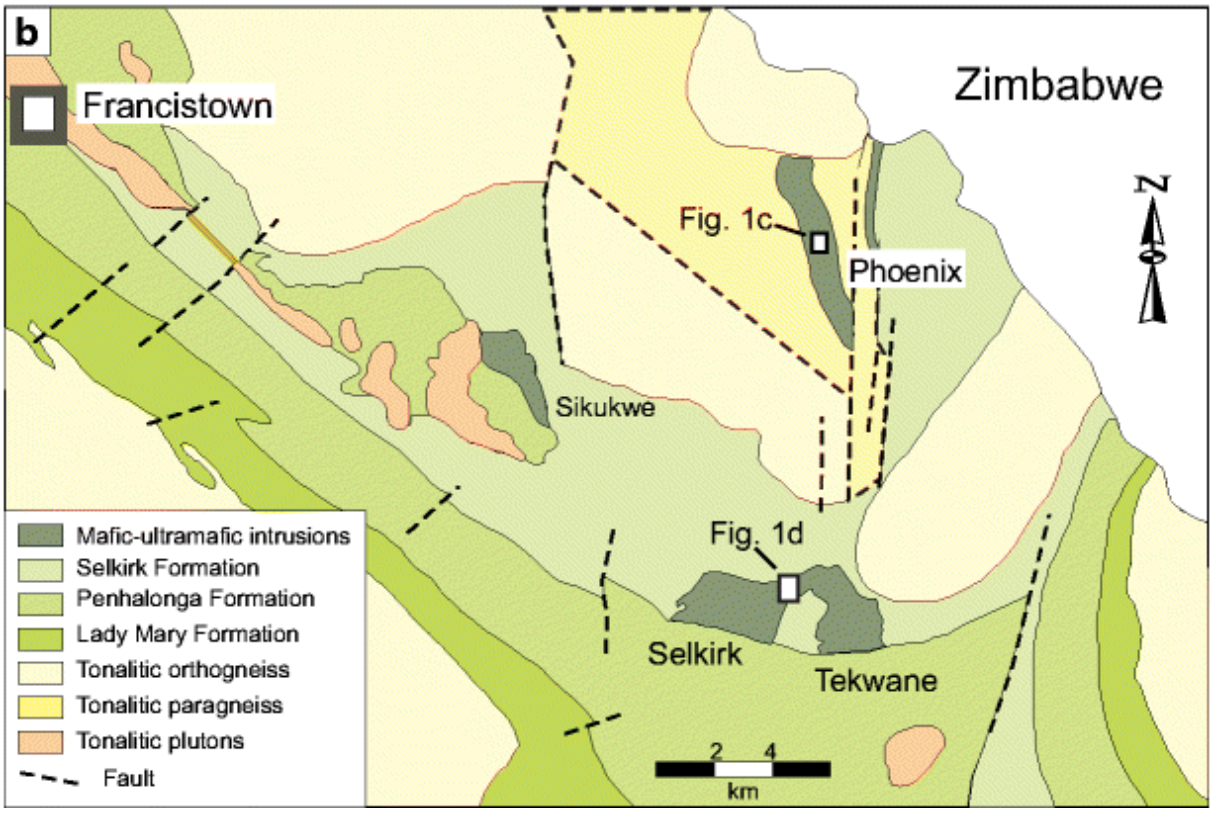

Figure 2.4: Continued.

2.1.4 Sudbury Igneous Complex, Canada

The Sudbury Igneous Complex, located in the Ontario Province of Canada is a Proterozoic geological feature well-known for its evidence of catastrophism, suggesting possible formation as a consequence of a meteorite impact (Rousell *et al.*, 2003). In mining and metallurgy, however, this deposit is well-known for its extensive nickel, copper and PGE reserves (1500 Mt at 1 % Ni, 1 % Cu, 1 g/t Pt, Pd; Farrow and Lightfoot, 2002). The Sudbury Igneous Complex is an oval shaped body 60 km long and 27 km wide as illustrated in figure 2.5. It is divided into an outer Main Mass and Sublayer with the surrounding Whitewater Group as basin in-fill (Naldrett and Kullerud, 1967; Farrow and Lightfoot, 2002). The northwest and southeast borders of the basin are more commonly known as the North and South Range, respectively. The terminology, Sudbury Igneous Complex is used here, but it should be mentioned that it is also referred to as Nickel Irruptive in some older literature e.g. Naldrett and Kullerud (1967). Rocks of the South Range are associated with the Proterozoic Huronian Supergroup sediments and volcanics whereas the North Range is associated with Archean gneisses (Keays and Lightfoot, 2004). The deposit can be further divided into the Main Mass, consisting of a lower norite, quartz gabbro and upper granophyre, and the Contact

Sublayer. The Contact Sublayer is an igneous breccia occurring discontinuously beneath the Norite and is in turn underlain by a metamorphic textured Footwall breccia.

Sulfide mineralisation in the Sudbury Igneous Complex has been recognised in four different environments as illustrated by figure 2.6. The first type of mineralisation is associated with the Contact Sublayer breccia. A second type occurs within the Footwall Breccia. A third type of mineralisation occurs in veins in the footwall. The last type of mineralisation is known as the Offset dykes and consists of sulfide mineralisation in quartz diorite dykes which may occur either as radial dykes extending away from the Complex, or as concentric dykes wrapped around the perimeter of the Complex (Farrow and Lightfoot, 2002; Keays and Lightfoot, 2004).

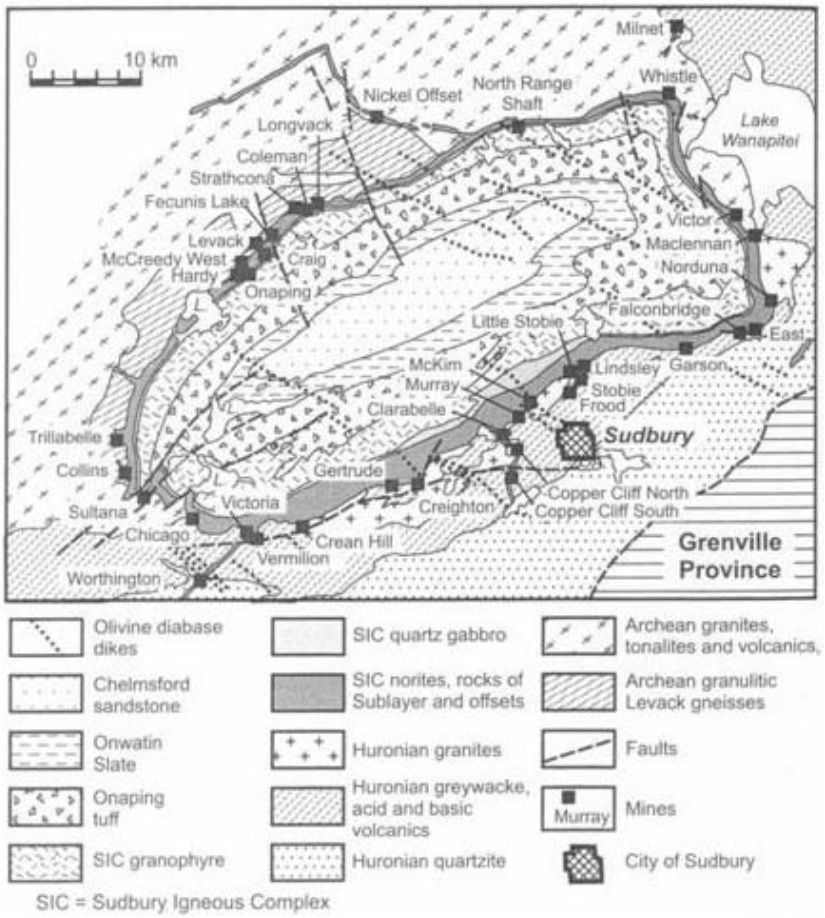

Figure 2.5: Geological map of the Sudbury Igneous Complex. From: Naldrett (2004).

The Gertrude pyrrhotite sample examined in this study is a typical Contact deposit occurring within the Footwall Breccia. The Gertrude site is marked by a distinct magnetic anomaly. The Gertrude mine was only recently reopened and is located just west of Creighton Mine in the South Range (Figure 2.5). The Gertrude ore body is tabular in shape and between 6 and 10 m in thickness with sulfides occurring as semi-massive, blebby and sometimes disseminated textures (E. Tremblay, Pers. Comm, 2007). The Contact type deposits typically have lower platinum group element grades relative to the Offset dyke type deposits. The Copper Cliff North (CCN) ore body examined in this study is a typical Offset dyke type deposit. The Copper Cliff Offset dyke extends for 7 km and strikes southwards from the South Range as shown in figure 2.5. It is subdivided into the North mine and South mine by the Creighton Fault. The ore body at Copper Cliff North mine is located within the centre of the dyke whereas, at Copper Cliff South mine, it is located at the edges of the dyke (Magyarosi *et al.*, 2002). Sulfide mineral textures present in the Copper Cliff ores include massive, semi-massive, blebby, net-textured and with rare disseminated sulfides (Rickard and Watkinson, 2001; Farrow and Lightfoot, 2002; Magyarosi *et al.*, 2002; Scott and Benn, 2002; Keays and Lightfoot, 2004).

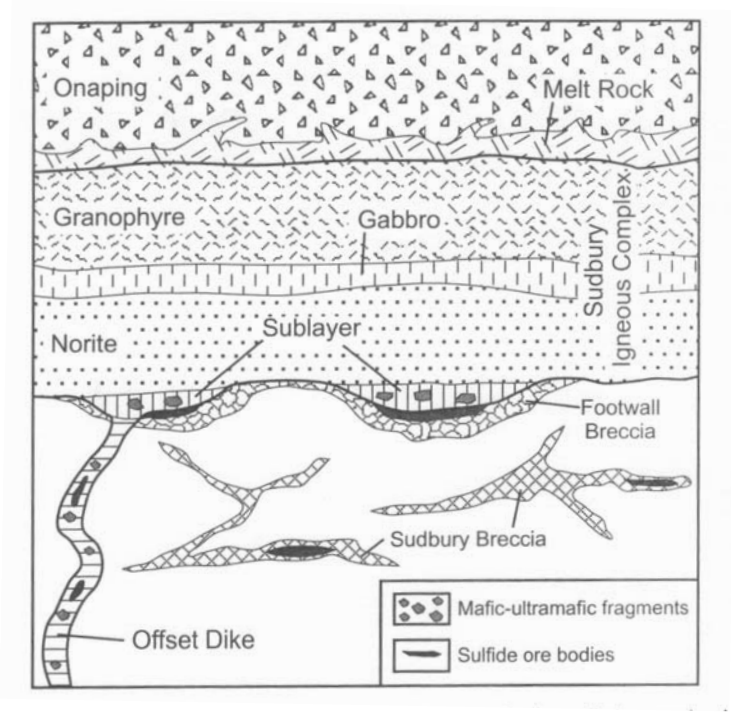

Figure 2.6: Vertical section showing the relationship between the Contact Sublayer and Offset dykes in the Sudbury structure. From: Naldrett (2004).

Dominant sulfides present within both Contact and Offset type deposits from mines of both the North and South Ranges are pyrrhotite, pentlandite, chalcopyrite, and minor sphalerite and magnetite displaying oxy-exsolution of ilmenite (Naldrett and Kullerud, 1967; Rickard and Watkinson, 2001; Farrow and Lightfoot, 2002; Magyarosi *et al.*, 2002; Keays and Lightfoot, 2004). The Offset dykes are generally more enriched in the platinum group elements than Contact deposits (Farrow and Lightfoot, 2002). Platinum group elements are mostly deported as discrete minerals with only minor elements in solid solution. Platinum group elements measured in solid solution in sulfides from the Contact type Strathcona deposit (Figure 2.5) include iridium, rhodium and ruthenium in pyrrhotite, whereas palladium was significantly enriched in pentlandite (Li *et al.*, 1993). The discrete platinum group minerals occurring in Sudbury ores are dominated by the tellurides (e.g. michenerite) and bismuth-tellurides (e.g. froodite) with distinct differences in platinum palladium mineral types between the North and South Ranges (e.g. sperrylite dominates in the South Range). Platinum group mineral sulfides are very rare, unlike the Bushveld Igneous Complex (Farrow and Lightfoot, 2002).

2.2 Pyrrhotite Mineralogy and Crystallography

2.2.1 Building blocks of pyrrhotite structures

The pyrrhotite group of minerals is based on the hexagonal structure of the mineral nickeline / niccolite (NiAs) and the nomenclature of the various pyrrhotite superstructures is based on the unit cell parameters of the NiAs structure (a =3.438Å, c = 5.880 Å; Wyckoff, 1963). Within this basic structure the metal atoms lie in a hexagonal lattice, whereas the non-metal atoms are positioned in a hexagonal close packed lattice. As shown in figure 2.7, nickel atoms are in octahedral coordination with the more electronegative arsenic atoms that are in trigonal prismatic coordination. One of the consequences of this structure is that the omission of metal atoms along certain crystallographic orientations is possible, thereby allowing the non-stoichiometry within the derivative pyrrhotite mineral group.

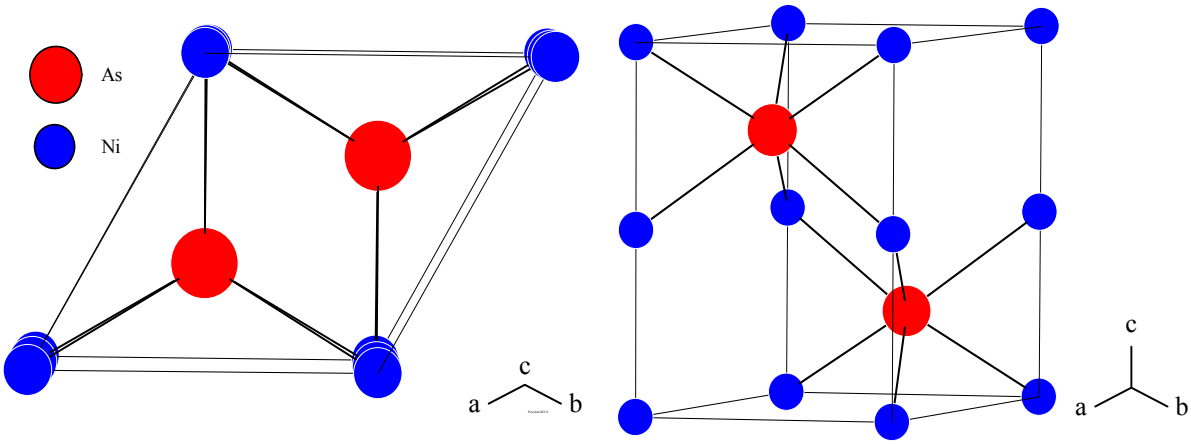

Figure 2.7: Illustration of the simple NiAs structure viewed in two orientations.

The pyrrhotite family consists of derivatives of the structure of the hexagonal NiAs subcell. These derivative structures are formed by extending the dimensions of the unit cell along the *c*-axis and are known as *superstructures*. These superstructures are non stoichiometric pyrrhotites varying in composition (Fe_7S_8 to $Fe_{11}S_{12}$), in crystal system, in mineral stability and in magnetic characteristics. These varying characteristics are essentially a function of the presence of metal cation vacancies in the pyrrhotite structure and the complexities associated with the stacking sequence of these vacancies, the repeat distance of the complete pattern and the direction of the vacancy layers within the superlattice. High temperature forms of

pyrrhotite are generally disordered and upon cooling, the iron site vacancies develop some order. Consequently, a number of pyrrhotite superstructures are developed such as those shown in table 2.2. In order to be able to describe these pyrrhotite superstructures, Wuensch (1963) introduced a nomenclature system whereby the superlattice dimensions are described according to the repeat of the NiAs unit cell either along the *a*-axis or *c*-axis. Accordingly a pyrrhotite with the structure and cell dimensions of NiAs is referred to as a 1C pyrrhotite, a pyrrhotite which has unit cell parameters of *c* equal to two times the dimension of *c* in the NiAs unit cell is known as 2C and corresponds to troilite, whereas 4C monoclinic pyrrhotite has unit cell parameters of *c* equal to four times the dimension of *c* in the NiAs unit cell.

Table 2.2: Summary of the different pyrrhotite varieties with some of their key physical attributes. See text for further description of the terminology used. Adapted from Posfai *et al.* (2000) and Fleet (2006).

Type	Comp.	Structure	Magnetic Properties	Other names	Stability	Occurrence	Refs
1C	FeS	Hex	pm	-	High temp phase	Synthetic	1, 2
2C	FeS	Hex	afm	Troilite	$<147^0$C	Natural & lunar	3-6
NC	Fe_9S_{10}, $Fe_{10}S_{11}$, $Fe_{11}S_{12}$	Hex, Ortho, Mon	afm	Non-magnetic, 5C, 6C, 11C, Intermediate pyrrhotite	$<209^0$C	Natural	2-3, 6-7
NA	Fe_7S_8	Trig	afm	2A, 3C	$< 262^0$C	Synthetic	2, 8-10
MC		Hex?	afm	-	$< 315^0$C	Synthetic	1, 2
4C	Fe_7S_8	Mon	fm	Magnetic Pyrrhotite	$< 254^0$C	Natural	3, 11-13
-	$Fe_{7+X}S_8$	Mon	afm	Anomalous Pyrrhotite	?	Natural	14

Note: pm – paramagnetic, afm – antiferromagnetic, fm - ferrimagnetic. [1] Nakazawa and Morimoto (1971) [2] Kissin and Scott (1982) [3] Morimoto *et al.* (1970) [4] Evans (1970) [5] Skala *et al.* (2006) [6] Fleet (2006) [7] Koto *et al.* (1975) [8] Francis and Craig (1976) [9] Nakano *et al.* (1979) [10] Keller-Besrest *et al.* (1982) [11] Bertaut (1953) [12] Tokonami *et al.* (1972) [13] Powell *et al.* (2004) [14] Clark (1966).

Following this nomenclature system, a number of pyrrhotite varieties or subgroups were identified based on some consideration of the stability of these phases within their experimental phase diagrams (Figure 2.8). A summary of the distinguishing physical properties of the pyrrhotite superstructures is given in table 2.2 along with the unit cell parameters and symmetry in table 2.3. The focus of this study however, will be on those pyrrhotite types that are naturally occurring (2C, NC, 4C) and are likely to be encountered in various mineral processing operations.

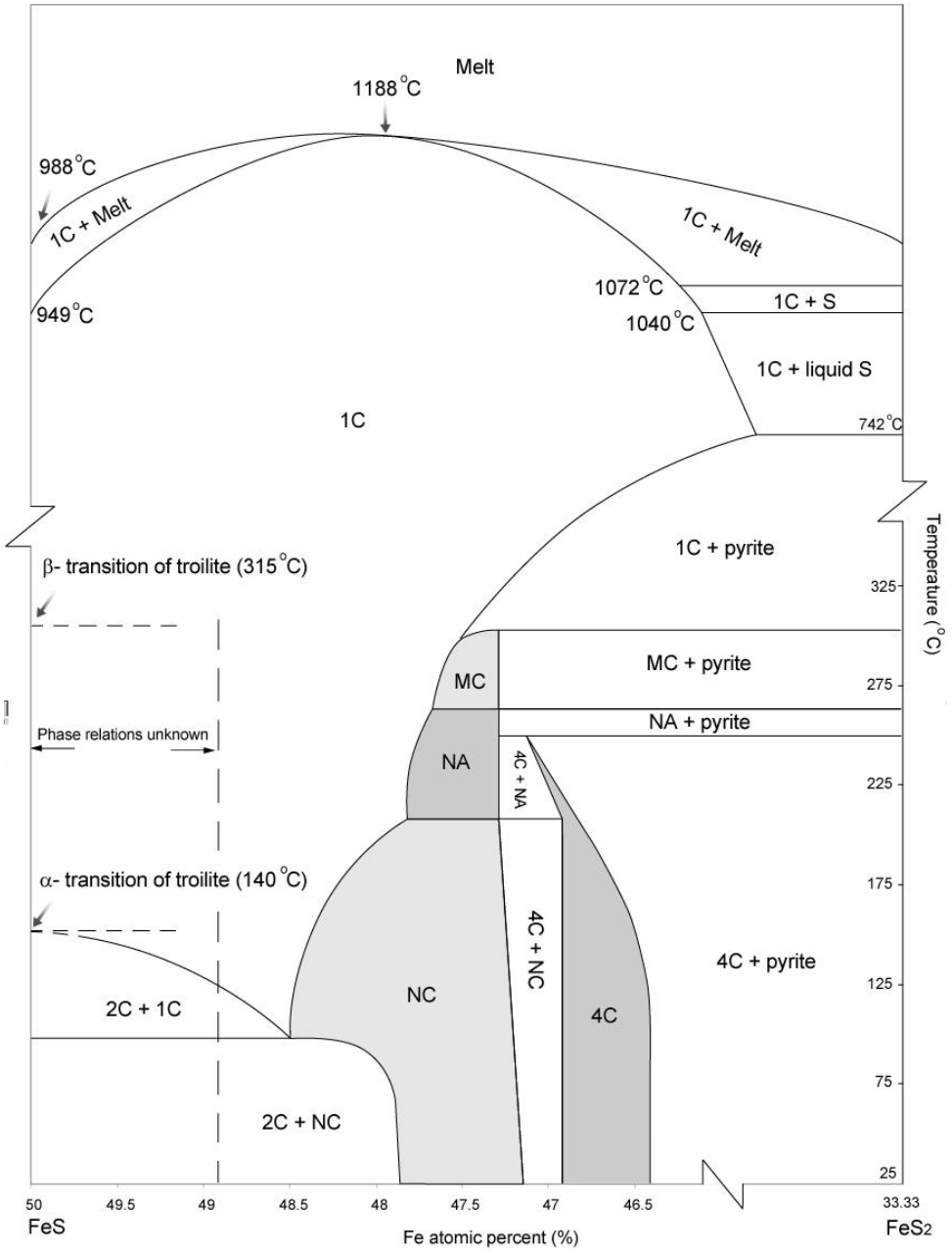

Figure 2.8: Phase diagram for the system FeS to FeS_2 representing stability fields of various pyrrhotite superstructures discussed in the text. From: Wang and Salveson (2005) and references therein.

Table 2.3: Summary of pyrrhotite superstructures and unit cell dimensions found in the literature.

Type	Comp.	Structure	Symmetry	a (Å)	b (Å)	c (Å)	β	Location	Refs
Nickeline	NiAs	Hex	$P\bar{6}3mc$	3.602	-	5.009	-	-	1
2C	FeS	Hex	$P\bar{6}2c$	5.962	-	11.750	-	Sea of Tranquility, Moon	2
2C	FeS	Hex	$P\bar{6}2c$	5.965	-	11.757	-	Etter Chondrite	3
3C	Fe_7S_8	Trig	$P3_1$	6.8673	-	17.062	-	Synthetic	4
3C	Fe_7S_8	Trig	$P3_121$	6.8652	-	17.046	-	Synthetic	5
3C	Fe_7S_8	Trig	$P3_121$	6.866	-	17.088	-	Synthetic	6
4C	Fe_7S_8	Mon	F2/*d*	11.902	6.859	22.787	90.26^0	Kisbanya, Romania	7
4C	Fe_7S_8	Mon	C2/c	11.926	6.882	12.925	118.02^0	Synthetic	8
5C*	Fe_9S_{10}	Hex	-	6.881	-	28.68	-	Ore Knob, N. Carolina	9
5C*	Fe_9S_{10}	Hex	-	6.88	-	28.7	-	Outokumpu, Finland	10
5C*	Fe_9S_{10}	Ortho	C*ca	6.8846	11.936	28.676	-	Kishu, Japan	11
6C*	$Fe_{11}S_{12}$	Hex	-	6.904	-	34.51	-	Merensky Reef, RSA	9
6C*	$Fe_{11}S_{12}$	Mon, pseudo-ortho	F*d* or F2/*d*	6.895	11.9536	34.518	90.00^0	Chigusa, Japan	12
11C*	$Fe_{10}S_{11}$	Ortho	Cmca or C2ca	6.892	11.952	63.184	-	Ongul, Antarctica	10

* Indicates no structure solution presented in these references. [1] Wyckoff (1963) [2] Evans (1970) [3] Skala *et al.* (2006) [4] Fleet (1971) [5] Nakano *et al.* (1979) [6] Keller-Besrest *et al.* (1982) [7] Tokonami *et al.* (1972) [8] Powell *et al.* (2004) [9] Carpenter and Desborough (1964), [10] Morimoto *et al.* (1970), [11] Morimoto *et al.* (1975b), [12] Koto *et al.* (1975).

2.2.2 Metastable 1C pyrrhotite

The 1C pyrrhotite is an undifferentiated, high temperature form of pyrrhotite (Figure 2.8) with a disordered distribution of vacancies (Nakazawa and Morimoto, 1971; Kissin and Scott, 1982). It has a structure similar to the NiAs type of structure, based on a single repeat of the NiAs unit cell along the c-axis (Nakazawa and Morimoto, 1971). 1C pyrrhotite is paramagnetic in character. Due to its limited occurrence only at higher temperatures e.g. the experimental studies of Nakazawa and Morimoto (1971) and Kissin and Scott (1982), or in a

9 km deep borehole from the German Deep Continental Drilling program (Posfai *et al.*, 2000), it is unlikely to occur in natural ore deposits and will not be discussed further.

2.2.3 2C Troilite

Stoichiometric FeS is more commonly known as troilite for which the structure is shown in figure 2.9. It is hexagonal, falls into space group $P\bar{6}2c$, can be described as a =√3A, and c = 2C where A and C are dimensions of the NiAs subcell. All metal cation sites are filled in the pyrrhotite structure and therefore troilite has an ordered structure with no vacancies. The ideal stoichiometric troilite is comprised of equal atomic proportions of ferrous iron and sulfide sulfur, although the findings of Skinner *et al.* (2004) suggested the presence of minor amounts of ferric iron in the troilite structure. Unlike the ideal trigonal prismatic coordination of arsenic in the NiAs structure, the sulfur atoms are more distorted and may even verge upon a deformed tetragonal scalenohedron, whereas the coordination of iron atoms remains relatively close to octahedral (Figure 2.9; Skala *et al*., 2006).

Troilite is antiferromagnetic in character at temperatures less than 140^0C at 1 bar, although it may undergo an α-magnetic phase transition, followed by a β phase transition at 315^0C (Curie temperature) where it transforms into the disordered 1C subcell of the NiAs structure (Figure 2.8; Fleet, 2006). The question of whether troilite undergoes a structural change associated with the α-magnetic phase transition is debatable (Wang and Salveson, 2005; Fleet, 2006).

Troilite is generally formed in reducing environments where ferrous iron is stable. Extraterrestrial occurrences are strongly reducing environments and consequently, troilite is well-known for its presence in lunar samples or meteorites (Evans, 1970; Bullock *et al.*, 2005; Skala *et al.*, 2006). However, this does not preclude its presence in some terrestrial locations, as fine lamellar intergrowths with non-magnetic pyrrhotite e.g. Merensky Reef, South Africa (Liebenberg, 1970) or Voisey's Bay, Canada (Naldrett *et al.*, 2000).

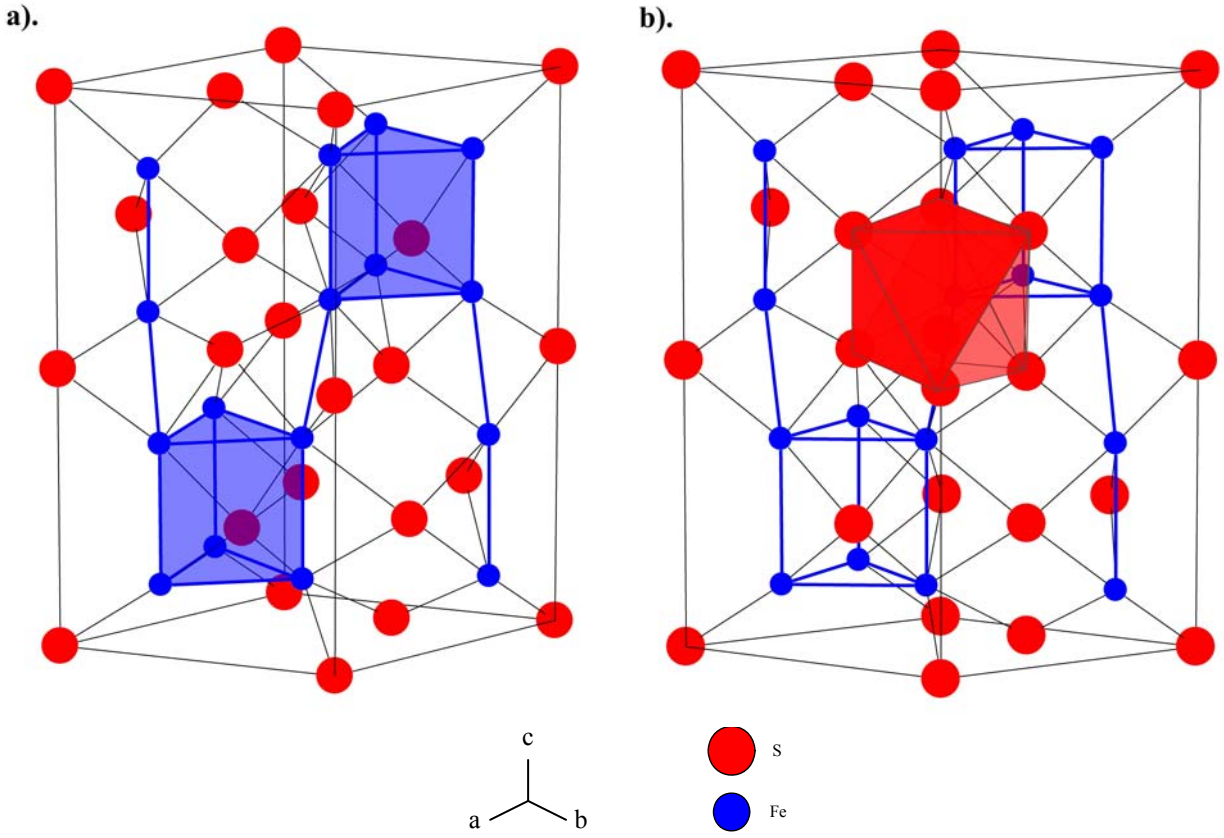

Figure 2.9: Illustration of the structure of lunar troilite. Blue lines represent Fe-Fe bonds, black lines represent iron sulfur bonds. The ideal coordination of sulfur in SFe_6 trigonal prisms is illustrated in (a) and coordination of iron in FeS_6 octahedra in (b). From: Evans (1970).

2.2.4 Metastable NA and MC pyrrhotites

Both the NA and MC pyrrhotite types are metastable existing in a relatively narrow temperature range between 209 and 308^{0}C (Figure 2.8; Kissin and Scott, 1982). The NA pyrrhotite is also sometimes known as 3C pyrrhotite due to the repeat distance of the *c*-axis representing three times that of the NiAs subcell (Francis and Craig, 1976). However, due to the presence of non-integral repeats along the *a*-axis of the NiAs unit cell, this pyrrhotite type is more correctly known as NA pyrrhotite (Nakazawa and Morimoto, 1971). The MC pyrrhotite is similar to NA pyrrhotite but with M non-integrally changing between 3 and 4 (Nakazawa and Morimoto, 1971). The NA and MC pyrrhotite superstructures represent a progressive ordering of vacancies with a decrease in temperature from the disordered 1C pyrrhotite. However, this still only represents a partial ordering of vacancies in comparison to the lower temperature 4C and NC structures where ordered vacancies exist (Keller-Besrest *et*

al., 1982; Makovicky, 2006). Due to the unlikely occurrence of these two pyrrhotite superstructures in natural ore deposits, they will not be discussed further.

2.2.5 Magnetic 4C pyrrhotite

The original monoclinic 4C pyrrhotite structure was proposed by Bertaut (1953) with unit cell parameters of a = 2√3A, b=2A, c = 4C where A and C represent the NiAs subcell dimensions. The 4C pyrrhotite superstructure is characterised by the distinct ordering of vacancy layers oriented along the *c*-axis. Individual vacancy containing layers are separated by completely filled metal cation layers in a sequence described as AFBFCFDF where A, B, C and D denote vacancy layers containing vacancies in the A, B, C, and D positions, and F, the completely filled iron layers as shown in figure 2.10. Within this structure a quarter of the iron atoms are absent and thus it has been proposed that charge balance is maintained by the presence of ferric iron in the pyrrhotite structure (Tokonami *et al*., 1972). Similarly to troilite, iron is in an octahedral coordination whereas sulfur is now in a combination of five fold and six fold coordination due to the presence of iron vacancies. More recent structure determinations of the 4C monoclinic pyrrhotite include that of Tokonami *et al.* (1972), although with the use of the unconventional space group F2/d that was originally used in the structure of Bertaut (1953). The unconventional unit cell was chosen to maintain an approximately orthogonal unit cell and to use nomenclature such that vacancy repeats are integral to the NiAs unit cell along the *c*-axis. Subsequently, Powell *et al.* (2004) determined the 4C structure with the use of powder neutron diffraction on a synthetic pyrrhotite sample and refined the structure in the C2/c space group. The relationship between the two space groups is shown in figure 2.11.

Monoclinic 4C pyrrhotite is ferrimagnetic and is therefore more commonly known as *magnetic pyrrhotite,* which is the choice of nomenclature for this study. The ideal composition of magnetic 4C pyrrhotite is Fe_7S_8 with a compositional range between 46.6 and 46.9 atomic % iron (Carpenter and Desborough, 1964). According to Bertaut (1953), the formula Fe_7S_8 can also be described as $Fe_2^{3+}Fe_5^{2+}S_8$ to account for the non-stoichiometry in the pyrrhotite structure. Bertaut (1953) also argued that the most stable energy configuration existed when the ferric iron cations were distributed over both the vacancy and full layers. According to the saturation magnetization from Powell *et al.* (2004) however, it is more likely that the ferric iron cations are restricted to the vacancy layers.

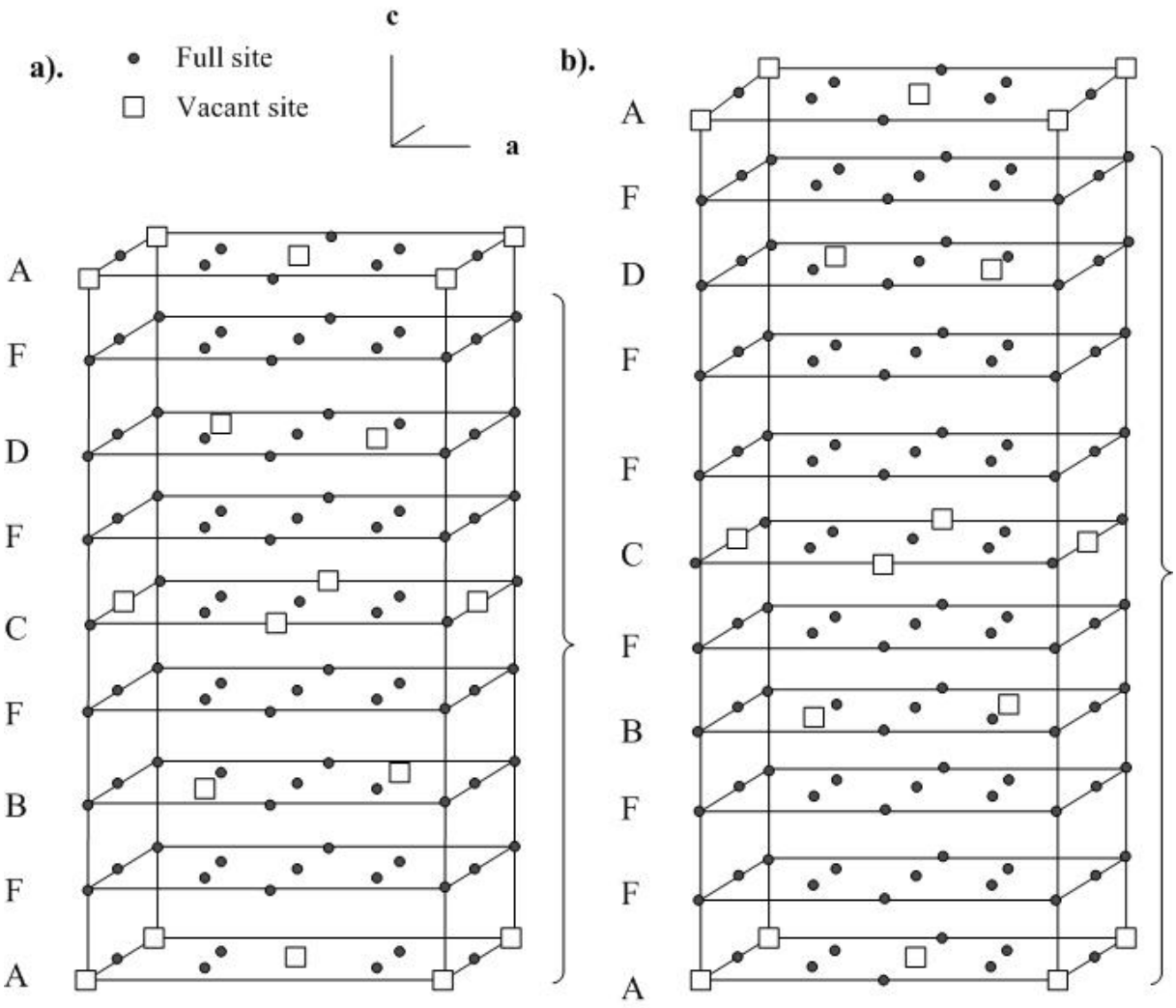

Figure 2.10: (a) Illustration of the vacancy structure in 4C magnetic pyrrhotite in the sequence AFBFCFDFA and based on the space group F2/d. (b) Illustration of the proposed vacancy structure for 5C pyrrhotite adapted from Vaughan *et al.* (1971). Sulfur sites are omitted for clarity.

However, the debate is still ongoing as to whether ferric iron even exists in the pyrrhotite structure. Mössbauer spectroscopy has not been a successful tool to recognise individual ferrous and ferric iron valence states in pyrrhotite due to the very rapid electron transfer, whereas both XANES and XPS have been successful. Pratt *et al.* (1994) used XPS on vacuum fractured monoclinic pyrrhotite to show the presence of both ferrous and ferric iron. Similarly, Mikhlin and Tomashevich (2005) showed the presence of ferric iron in monoclinic pyrrhotite using XANES. In contrast, Letard *et al.* (2007) used XMCD to study pyrrhotite and argued that only ferrous iron is present in pyrrhotite.

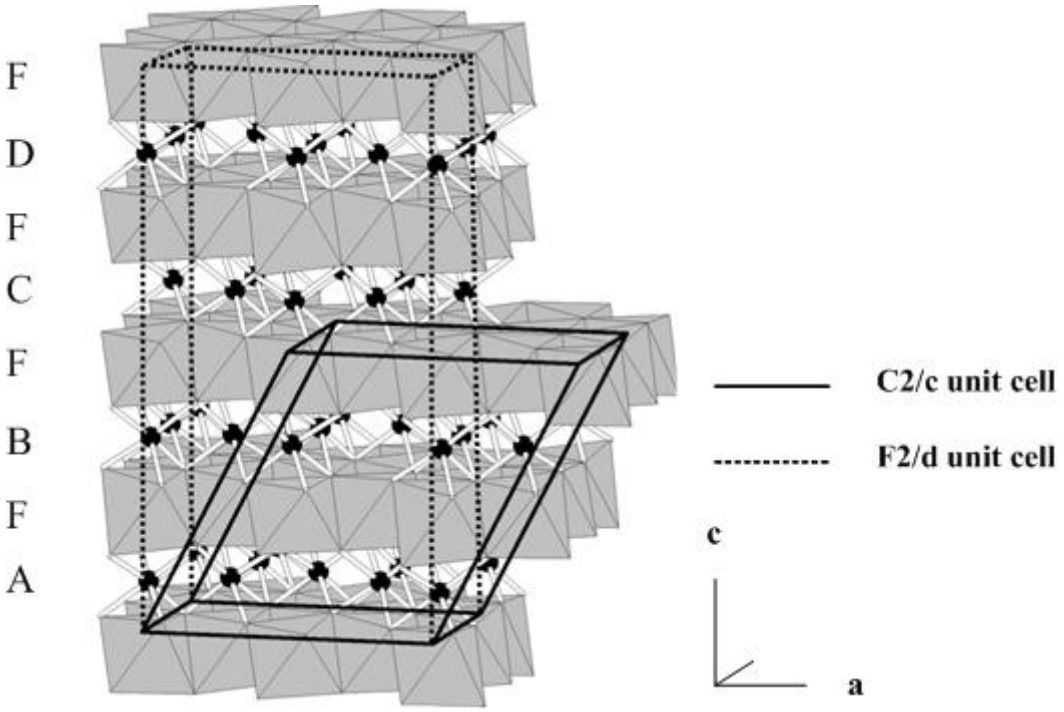

Figure 2.11: (a) Illustration of the relationship between the F2/d and C2/c space groups as used by Tokonami *et al.* (1972) and Powell *et al.* (2004), respectively, in describing the structure of magnetic 4C pyrrhotite. Iron sites are illustrated as solid circles in vacancy layers and as shaded octahedra in fully occupied layers. Adapted from: Powell *et al.* (2004).

According to the pyrrhotite phase relations shown in figure 2.8, magnetic 4C pyrrhotite is stable below 254^0C (Kissin and Scott, 1982) and may co-exist with either NC pyrrhotite (more iron rich bulk compositions) or with pyrite (more sulfur rich compositions). The phase relations also suggest that the 4C monoclinic pyrrhotite is the lower temperature, more ordered form of pyrrhotite derived from NA pyrrhotite. Since primary magnetic 4C pyrrhotite and troilite are incompatible, it suggests that where magnetic pyrrhotite and troilite do co-exist, the role of secondary alteration or oxidation needs to be evaluated (Liebenberg, 1970; Lianxing and Vokes, 1996).

4C magnetic pyrrhotite is one of the most commonly documented pyrrhotite forms in natural terrestrial occurrences. Both Carpenter and Desborough (1964) as well as Arnold (1967) demonstrated the abundance of 4C pyrrhotite types in their respective studies of pyrrhotite from different geographic locations around the world. However, Arnold (1967) also showed that naturally occurring mixtures of 4C and NC pyrrhotite were far more frequent (73% of the samples analysed) and this has been verified by numerous other studies of pyrrhotite

occurrences (e.g. Naldrett and Kullerud, 1967; Liebenberg, 1970; Lianxing and Vokes, 1996; Posfai *et al.*, 2000).

An anomalous monoclinic pyrrhotite of composition $Fe_{7+x}S_8$ has also been described in the literature by Clark (1966). Anomalous pyrrhotite appears to be common in low-temperature sedimentary environments and is antiferromagnetic unlike normal monoclinic pyrrhotite that is ferrimagnetic.

2.2.6 Non-magnetic NC pyrrhotite

NC pyrrhotite, also known as intermediate or *non-magnetic* pyrrhotite consists of a series of pyrrhotite superstructures. These are generally grouped together for simplicity during phase relationship studies (e.g. Nakazawa and Morimoto, 1971) and are shown in tables 2.2 and 2.3. The value of N, representing the repeat distance of the *c*-axis dimension of the NiAs subcell may be both integral and non-integral, varying between 5 and 11. The integral NC superstructures of pyrrhotite can be linked to their ideal composition using the relationship of Morimoto *et al.* (1970) where: $Fe_{n-1}S_n$ (n>8). If *n* is even then the structure is *n*/2C (ie. 5C pyrrhotite with composition Fe_9S_{10}, 6C pyrrhotite with composition $Fe_{11}S_{12}$) or if *n* is odd then the structure is *n*C (ie 11C pyrrhotite with composition $Fe_{10}S_{11}$). Solid solutions between the compositions Fe_9S_{10} to $Fe_{10}S_{11}$, and between $Fe_{10}S_{11}$ and $Fe_{11}S_{12}$ are considered to be metastable, although they may result in some of the non-integral or incommensurate periodicities of N identified in some studies (e.g. N = 5.38, 5.5, 5.7, 6.6, 10, 28; Pierce and Buseck, 1974; Morimoto *et al.*, 1975a; Posfai *et al.*, 2000).

The exact ordering of vacancies in the non-magnetic NC structure is rather complex and hence no complete crystal structure solutions exist in the literature. This does not preclude that some have postulated ideal vacancy distributions based on the 4C monoclinic structure (e.g. Vaughan *et al.*, 1971; Nakazawa and Morimoto, 1971; Posfai and Dodony, 1990). Since the absolute number of vacancies is theoretically fixed for the integral NC pyrrhotites, by inserting additional filled iron layers into the 4C structure, potential vacancy distributions can be proposed. Vaughan *et al.* (1971) proposed a structure alternating between one and two filled layers for the 5C pyrrhotite as shown in figure 2.10. For the 6C pyrrhotite Nakazawa and Morimoto (1971) suggested a vacancy layer at every third iron layer whereas Koto *et al.*

(1975) argued that the vacancy distribution for 6C pyrrhotite was probably not ideal and consisted of some half filled iron sites alternating with fully occupied iron sites.

As shown by table 2.3, the crystallography of the non-magnetic NC pyrrhotites is debatable with accounts of the 5C pyrrhotite described as hexagonal or orthorhombic, the 6C pyrrhotite described as hexagonal, monoclinic or pseudo-orthorhombic, and the 11C pyrrhotite as orthorhombic (Carpenter and Desborough, 1964; Morimoto *et al.*, 1970; Koto *et al.*, 1975; Morimoto *et al.*, 1975b). Since the apparent x-ray diffraction symmetry of the NC pyrrhotite subcell is hexagonal, non-magnetic pyrrhotite has been termed "hexagonal" in the past for ease of reference (Posfai *et al.*, 2000).

Similarly, to the representation of the magnetic 4C pyrrhotite structure as a mixture of both ferric and ferrous iron, the non-magnetic NC pyrrhotites can be represented as follows; $Fe_7^{2+}Fe_2^{3+}S_{10}^{2-}$, $Fe_8^{2+}Fe_2^{3+}S_{11}^{2-}$, $Fe_9^{2+}Fe_2^{3+}S_{12}^{2-}$. The absolute amount of ferric iron is constant in the NC pyrrhotite but the overall proportion varies such that the 5C pyrrhotite has more ferric iron than the 11C and so forth. Mikhlin and Tomashevich (2005) also showed the presence of ferric iron in the "hexagonal" pyrrhotite structure using XANES. The non-magnetic NC pyrrhotite is antiferromagnetic.

Non-magnetic NC pyrrhotite is stable at temperatures less than 209^0C as shown by figure 2.8 and within this stability field, the type of NC superstructure formed is dependent upon both temperature and composition (Nakazawa and Morimoto, 1971). As to whether the non-integral NC pyrrhotite is metastable at ambient conditions or not, is a subject of debate in the literature, but this does not negate the observation that for some natural occurrences, the non-integral NC superstructures are far more abundant than integral NC superstructures (Morimoto *et al.*, 1970; Morimoto *et al.*, 1975b).

The iron content of the non-magnetic NC group of pyrrhotite superstructures at ambient conditions, has been found to vary between 47.0 and 48.0 atomic % iron (Carpenter and Desborough, 1964). The NC pyrrhotite can also coexist with 4C monoclinic pyrrhotite at more sulfur rich bulk compositions. However, for more iron rich bulk compositions with greater than 48 atomic % iron, troilite and NC pyrrhotite can coexist with one another (Figure 2.8). In natural occurrences, this has been observed as troilite exsolution lamellae from an NC pyrrhotite matrix (e.g. Gain and Mostert, 1982). Similarly, for more sulfur rich bulk

compositions, intergrowths of NC and 4C pyrrhotite are expected (e.g. Carpenter and Desborough, 1964; Naldrett and Kullerud, 1967; Lianxing and Vokes, 1996). However, the phase diagrams also suggest that there is a compositional stability field in which NC pyrrhotite exists by itself, which is borne out by descriptions of pure "hexagonal" pyrrhotite occurrences (Carpenter and Desborough, 1964; Arnold, 1967).

2.2.7 Relationship between pyrrhotite, pentlandite and the platinum group elements

Relationship between pyrrhotite types

In the past there have been many accounts describing the intergrowths between non-magnetic NC and magnetic 4C pyrrhotite. These have been performed using a variety of techniques in conjunction with optical microscopy such as the chromic acid etch and magnetic colloid method (e.g. Naldrett and Kullerud, 1967). In order for the description of pyrrhotite petrography in this study to be more meaningful, a summary of the types of intergrowth textures described in the literature is given along with the schematic of intergrowth textures in figure 2.12. This summary is based on the work of Lianxing and Vokes (1996), which characterised the textures of a variety of Norwegian pyrrhotites including those typical of magmatic nickel deposits.

Lianxing and Vokes (1996) classified the magnetic and non-magnetic pyrrhotite examined in their study into two groups; comprising "crystallographically controlled lamellar intergrowths" and "fissure controlled irregular intergrowths". The former were interpreted to represent textures controlled through primary ore forming processes involving pyrrhotite formation and annealing, whereas the latter were likely the result of secondary processes such as hydrothermal alteration (Desborough and Carpenter, 1965). There are several manifestations of the lamellar intergrowths of the crystallographically controlled magnetic pyrrhotite exsolved from non-magnetic pyrrhotite. All these manifestations are based on the interaction between multiple lamellae of magnetic pyrrhotite through processes such as annealing (Brady, 1987) and are summarised in figure 2.12. As shown in figure 2.12, the crystallographically controlled textures may consist of parallel lamellae of magnetic pyrrhotite hosted by non-magnetic pyrrhotite (a), thickness zonation (b), development of box work texture (c) or composite lamellae (d). The magnetic colloid may also highlight the

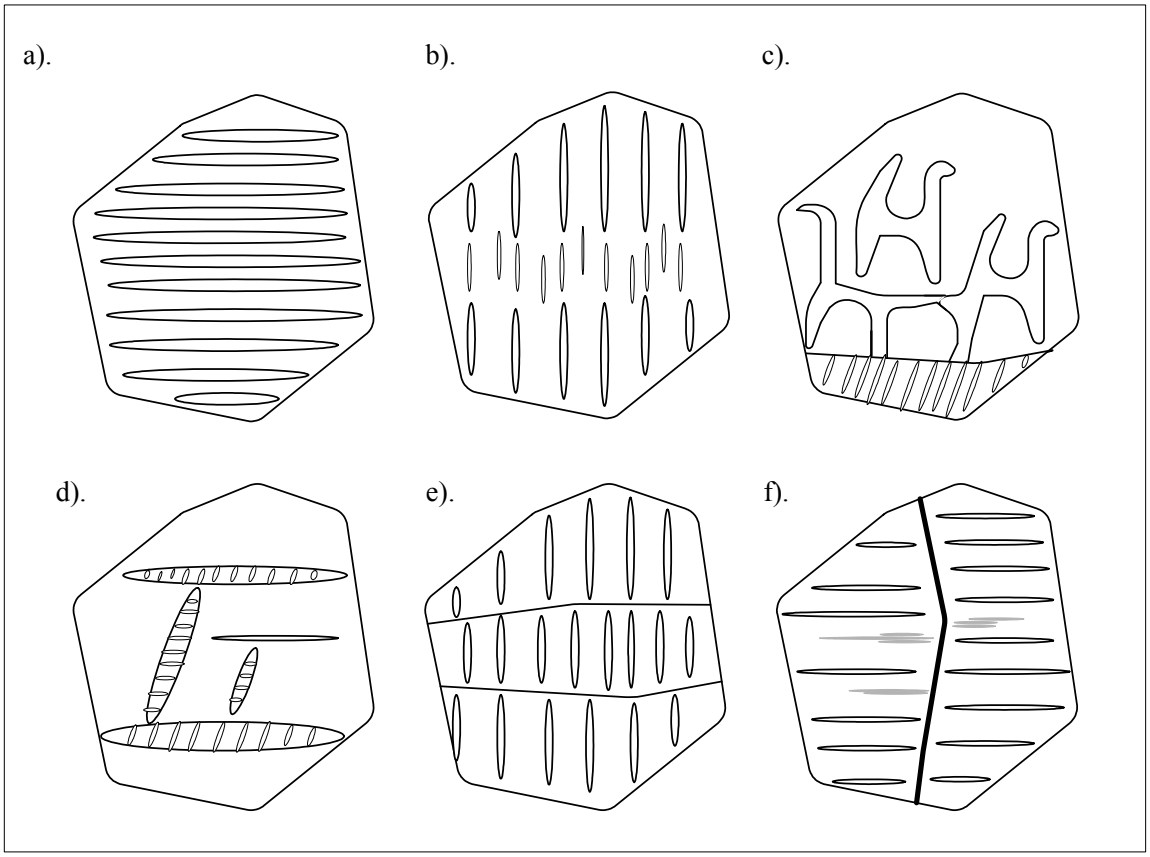

Figure 2.12: Graphical illustration of the types of crystallographically controlled intergrowths found in pyrrhotite. (a) Exsolution lamella of magnetic pyrrhotite hosted by non-magnetic pyrrhotite. (b) Thickness zonation of magnetic pyrrhotite lamellae hosted by non-magnetic pyrrhotite. (c) Box work textures of magnetic pyrrhotite hosted by non-magnetic pyrrhotite. (d) Composite lamellae of magnetic pyrrhotite hosted by non-magnetic pyrrhotite. (e) Magnetic domain walls in pyrrhotite. (f) Exsolution of pentlandite flames (grey) from fissure. Note that the orientation of the flames is parallel to the magnetic pyrrhotite exsolution lamellae. Adapted from photomicrographs in Lianxing and Vokes (1996) and Yamamoto *et al.* (1959).

location of magnetic domain walls (e). The second texture of "fissure controlled intergrowths" consists of irregular intergrowths of magnetic pyrrhotite blades and patches hosted along fissures and grain boundaries of non-magnetic pyrrhotite (Lianxing and Vokes, 1996).

Relationship between pyrrhotite and pentlandite

Due to the similarity in physical and chemical properties between iron and nickel cations in a thermo-chemical system, the behaviour of these two elements needs to be considered together. Practically, this means that the valuable nickel mineral, pentlandite, almost ubiquitously occurs with pyrrhotite, which has significant implications for mineral processing. Consequently, there has been much research in the past on understanding this

interrelationship in the Fe-Ni-S system. The work has generally focussed on the type example of the Sudbury magmatic sulfide deposit in Canada.

Pentlandite is classified as a metal sulfide with an excess of metal to sulfur. It is a solid solution between both iron and nickel with an ideal composition of $(FeNi)_9S_8$, is cubic in character and is based on a structure of metal-sulfur tetrahedra (Makovicky, 2006). Pyrrhotite and pentlandite both form from a high temperature immiscible Fe-Ni-S sulfide solid solution, more commonly know as the monosulfide solid solution or *MSS*. According to the phase diagram studies of Sugaki and Kitakaze (1998), at temperatures between 865 and 584^0C a high form of pentlandite exsolves from the MSS. This high pentlandite has half the size of the unit cell of low temperature pentlandite. Upon further cooling to below 615^0C, high pentlandite transforms into pentlandite *sensu stricto*. Textural forms of pentlandite which have been described for the Sudbury deposit include (Naldrett *et al.*, 1967; Naldrett and Kullerud, 1967; Kelly and Vaughan, 1983):

i). Blades of pentlandite along rims of pyrrhotite grain boundaries. The bladed texture tends to be replaced by a more granular pentlandite at triple junctions of pyrrhotite grain boundaries.
ii). Flame (lamellae-like) structures of pyrrhotite developed at grain boundaries or *en échelon* along fractures (Figure 2.12f).
iii). Flame structures of pentlandite hosted by a pyrrhotite matrix and unrelated to any structural defects.
iv). Occurrence of monoclinic pyrrhotite as rims around flame pentlandite.

These textural forms of pentlandite were recreated in the experimental studies of Kelly and Vaughan (1983) at 400^0C and were subsequently explained through the following mechanisms. The key however, was the dependence of pentlandite texture on the metal / sulfur ratio and cooling rate of the *MSS* as shown in figure 2.13 During the formation of pentlandite, clusters of iron and nickel atoms agglomerate and nucleate from the *MSS*. Due to the free energy of the system, these clusters prefer to nucleate along zones of structural defects such as grain boundaries and fractures. Further nucleation results in the gradual formation of continuous rims of pentlandite blebs or grains along pyrrhotite grain boundaries (i). Continual nucleation, especially for bulk compositions with higher metal to sulfur ratios results in the formation of finer blades or flames on grain boundaries or *en échelon*

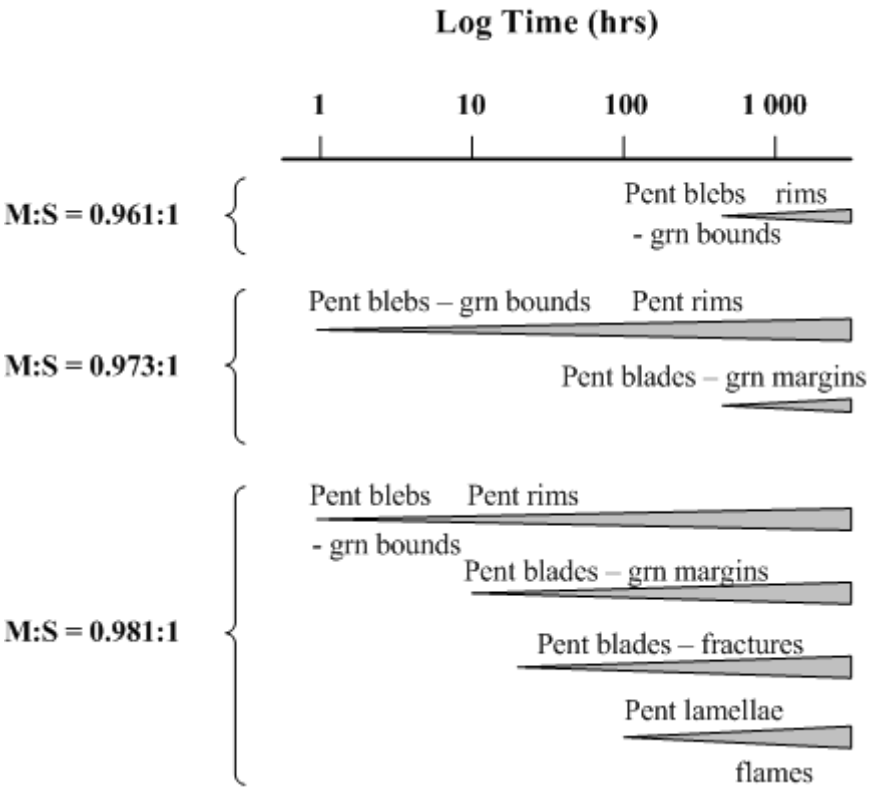

Figure 2.13: Relationship between the initial metal to sulfur ratio of the MSS and time in the formation of different pentlandite morphologies, based on an iron / nickel ratio of 5. "Grn bounds" represents pentlandite on grain boundaries, and "grn margins" represents the development of pentlandite on grain margins. From: Kelly and Vaughan (1983).

distribution along fractures (ii). With further cooling below ~240^{0}C, the diffusion rates decrease, and pentlandite nucleation is impaired, resulting in the formation of flames, unrelated to any defects. Crystallographic control may still exist resulting in the formation of these pentlandite flames in a direction perpendicular to the basal plane of the pyrrhotite (iii). Within these localised areas of flame pentlandite formation, the adjacent areas to the flames remain as nickel poor, sulfur rich sites causing the preferential formation of monoclinic pyrrhotite as rims to the flames (iv).

In addition to the formation of discrete pentlandite grains or flames, some residual nickel may occur in the pyrrhotite structure. Analyses of the residual concentration of nickel in "hexagonal" and monoclinic pyrrhotites from the Sudbury district, have shown that "hexagonal" pyrrhotites are more nickel rich (0.68 - 1.01 wt %) relative to the monoclinic pyrrhotite (0.35 - 0.5 wt %; Vaughan *et al.*, 1971; Batt, 1972).

Relationship between pyrrhotite and the platinum group elements

Some mention of the relationship between the platinum group elements and pyrrhotite should be made given that for some mineral processing operations, nickel is a by product of the beneficiation of the platinum group elements e.g. Merensky Reef, South Africa. This association is notable for magmatic sulfide deposits, although the Norilsk nickel deposits are also known to have measurable platinum group minerals (Cabri *et al.*, 2003). Experimentally derived partition coefficients show that the platinum group elements are more than 10 000 times more soluble in a sulfide liquid than the coexisiting basaltic liquid at high temperature (Crockett *et al.*, 1997). Upon cooling, the platinum group elements may remain in solid solution with minerals such as pentlandite or pyrrhotite. According to Ballhaus and Ulmer (1995), the 1C pyrrhotite structure can accommodate platinum and palladium in iron sites, but only when the occupied site is surrounded by 4 (Pd) or 5(Pt) vacancies in the crystal structure. Alternatively, discrete platinum group minerals may form through fractional crystallisation from the MSS.

2.2.8 Analytical methods for discrimination between pyrrhotite types

The need for an adequate methodology to be able to measure and quantify the textural relationship between magnetic and non-magnetic pyrrhotite types exists, since Arnold (1967) demonstrated that over 70 % of the pyrrhotite samples examined in his study were mixtures of "hexagonal" or non-magnetic pyrrhotite with monoclinic or magnetic pyrrhotite. These pyrrhotite types typically form a complex array of intergrowth textures such as those shown in figure 2.12. It is therefore apt in this process mineralogy study to review past methods as well as evaluate modern mineralogical analysis techniques which show potential for discrimination and quantification of the relationship between pyrrhotite types.

Optical microscopy based methods

The relationship between pyrrhotite types can be investigated based on differences in the optical and / or physical properties of magnetic and non-magnetic pyrrhotite using standard optical microscopy. In the study of Carpenter and Bailey (1973), troilite, "intermediate" and monoclinic pyrrhotite were differentiated entirely based on their inherent optical properties: reflectivity, tarnishing and angle of apparent rotation. It was shown that mineral structure had a greater influence on the optical properties (especially reflectivity) of pyrrhotite than

composition. Although Carpenter and Bailey (1973) were able to accurately distinguish between pyrrhotite types, the method used was highly specialised and appears not to have been used by their contemporaries.

Chromic acid etching techniques were more commonly used by others such as Ramdohr (1969), Graham (1969) and Naldrett *et al.* (1967) whereby etching caused one phase to be darker than the other. However, in some scenarios the non-magnetic pyrrhotite was the darker phase and magnetic pyrrhotite the lighter phase and in other cases, vice versa (Naldrett *et al*., 1967; Craig and Vaughan, 1981). An alternative method based on exploitation of the magnetic properties of ferrimagnetic monoclinic pyrrhotite has also been used. This has been known as "Bitter patterns" (Bitter, 1932), "powder patterns" (Zapletal, 1969) and more recently as the "magnetic colloid" method (Craig and Vaughan, 1981; Lianxing and Vokes, 1996). When the magnetic colloid method is used, magnetite particles suspended in a soapy solution aggregate in areas of the surface of the mineral where the greatest inhomogeneities exist in the magnetic field (Zapletal, 1969).

The strength of the magnetic colloid method is that once the colloid has been made and pyrrhotite samples prepared as polished ore mounts, it is a relatively quick, easy and inexpensive task to discriminate between pyrrhotite types. The inherent weaknesses in this method are that the observer needs to have some training in ore petrography in order to interpret the data. The response of pyrrhotite to the acid etch or colloid may also differ within an occurrence due to the varying surface reactivity of grains in varying orientations (Graham, 1969; Zapletal, 1972). In order to quantify the relative proportions of pyrrhotite types, methods such as point counting, which is subject to human error or image analysis would have to be used.

Crystallographic based methods

The primary means for the identification of pyrrhotite types is based upon their crystallographic properties. A number of fundamental analytical techniques have been used in the past in order to discriminate between pyrrhotite types and these include single crystal and precession camera x-ray methods as well as HRTEM (Morimoto *et al.*, 1970; Pierce and Buseck, 1974). Traditionally when single crystal x-ray information is examined, two types of information are obtained:

i) Geometry of all major spots or reflections derived from the interaction of the x-ray beam with the pyrrhotite single crystal
ii) Intensity of all major spots or reflections derived from the interaction of the x-ray beam with the pyrrhotite single crystal

By analysis of the geometry of all the major spots or reflections of the crystal, information on crystal lattice parameters and crystal symmetry is obtained. Once the crystal lattice parameters are known, the pyrrhotite superstructure can be deduced based on the length of the *c*-axis. The arrangement and number of weak spots derived from the superstructure reflections can also be used to confirm the pyrrhotite superstructure.

By analysis of the intensity of all the major spots or reflections of the crystal, the exact position of iron and sulfur atoms, as well as the position of vacant sites in the pyrrhotite crystal can also theoretically be determined. Due to the complexity of the pyrrhotite structure with respect to the ordering of vacancies as well as the lack of suitable pyrrhotite single crystals, complete structure solutions of pyrrhotite are quite limited. As shown in table 2.3, the majority of crystal structure solutions which exist are based on the analysis of synthetic specimens. To date, no complete crystal structure solution exists for non-magnetic NC pyrrhotite.

Single crystal x-ray diffraction (XRD) is however, too specialised for the routine measurement of pyrrhotite and is limited to single crystals. Consequently, powder x-ray diffraction methods are preferred, particularly since they are more representative of the bulk sample. The method described by Graham (1969) is based on the relative ratios of the characteristic pyrrhotite peaks in a powder x-ray diffractogram. This appears to have been the accepted method for many years in the nickel processing industry (e.g. A. Kerr, Pers. Comm. 2008). This method is based upon the differences in intensity between characteristic pyrrhotite peaks; magnetic pyrrhotite has a doublet at d = 2.066 and 2.056 Å, whereas non-magnetic pyrrhotite has a singlet at 2.066 Å, and troilite has a singlet at d = 2.094 Å as shown in figure 2.14. Comparison of the ratios of these characteristic pyrrhotite peaks with an external calibration curve, allows one to calculate the relative proportions of each pyrrhotite phase. More recently with the advent of XRD software using the Rietveld method for phase quantification based on the refinement of crystal structures using information obtained from an entire diffractogram as opposed to the characteristic pyrrhotite

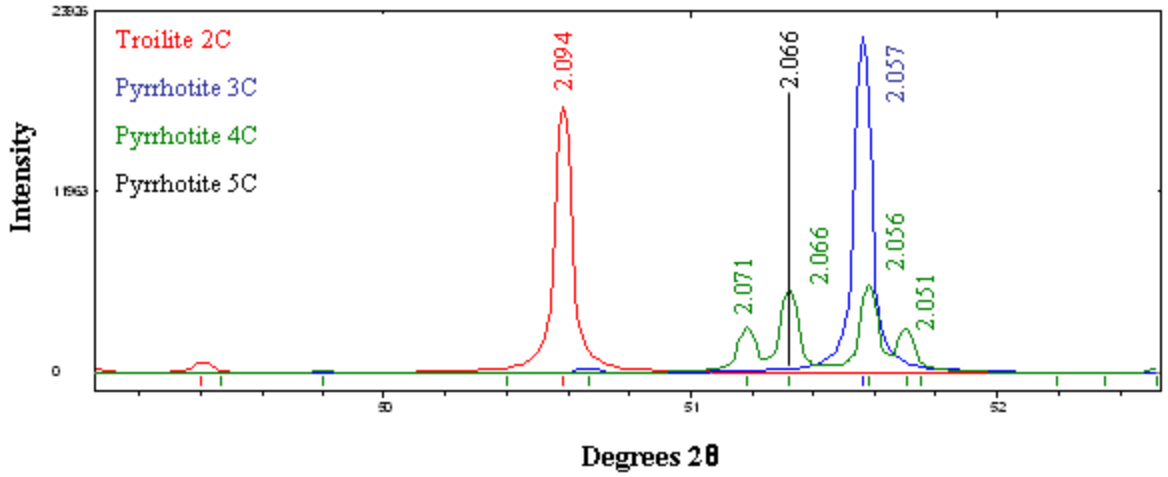

Figure 2.14: Comparison of the characteristic powder diffraction peaks of synthetic 3C hexagonal pyrrhotite, synthetic 4C magnetic, monoclinic pyrrhotite and natural 2C troilite based on the structures of Keller-Besrest *et al.* (1982), Powell *et al.* (2004) and Skala *et al.* (2006). The characteristic peak of 5C non-magnetic pyrrhotite based on the d-spacing of Carpenter and Desborough (1964) is also shown.

peaks, the relative proportions of the two pyrrhotite phases can in theory, be routinely determined in an unknown sample (Young, 1995; Raudsepp *et al.*, 2002; De Villiers and Verryn, 2008).

Strengths associated with the measurement and quantification of pyrrhotite in mixed samples with the powder XRD method are that both the sample preparation and measurement times are relatively quick and the cost of the analysis is moderate. Powder XRD methods are likely to be more statistically representative of the whole if samples are prepared following accepted sampling practice. However, the Rietveld method is based on upon the availability of appropriate crystal structure information. As shown in table 2.3, no complete crystal structure solution exists for non-magnetic NC pyrrhotite which is a significant short fall for the technique. Assuming the presence of suitable pyrrhotite crystal structures however, quantitative determination of the relative proportions of pyrrhotite types is restricted by the detection limits of the technique (~ 5 wt %). This may exclude the use of quantitative XRD for analysis of low grade ore deposits unless some upgrading of the sulfide component has been made.

Electron beam based methods

Electron beam based methods used for the differentiation of pyrrhotite forms may essentially be divided into those based upon the precise measurement of chemical composition or through the measurement of the average atomic number of the pyrrhotite sample based on its back scattered electron (BSE) signal. The electron microprobe (EMP) is ideal for spot analysis of the exact chemical composition of pyrrhotite which can be added to a dataset of magnetic and non-magnetic pyrrhotite compositions. However, proper calibration and standardisation is of the utmost importance to ensure the ability to be able to distinguish between the subtle differences in iron and sulfur contents. Since the EMP is a fairly specialised instrument, it is more appropriate to evaluate the potential contribution of a scanning electron microscope (SEM) for routine analysis of pyrrhotite types.

The SEM is an ideal instrument for using the BSE signal as a means to discriminate between pyrrhotite types. The BSE grey level of non-magnetic Fe_9S_{10} pyrrhotite is ~ 43.33 and is only just a little higher than magnetic Fe_7S_8 pyrrhotite, where the BSE grey level is ~ 43.16. Using this subtle difference in the BSE grey level, one can theoretically differentiate between magnetic and non-magnetic pyrrhotite phases under ideal imaging conditions. Zapletal (1969) performed a thorough study comparing pyrrhotite textures obtained using a SEM with those from the magnetic colloid and chemical etch techniques. In general, good correlation was determined between all the methods, but it was observed that the BSE signal was also subject to the effects of crystal orientation. To date, discrimination of pyrrhotite types based on their BSE signal appears not to have been developed for routine use.

With the advent of modern automated mineralogical techniques based on the scanning electron microscope such as the QEMSCAN or MLA, there is potential to develop a technique for analysis of magnetic and non-magnetic pyrrhotite. This could be routinely applied on metallurgical samples and provide rapid, automated quantitative mineralogical analysis between pyrrhotite types. The use of QEMSCAN or MLA is considered a prospective method for the discrimination between pyrrhotite phases and is accordingly further developed in this study (Section 3.3).

2.3 Electrochemical Properties of Pyrrhotite

The sulfide minerals are known to be prone to anodic oxidation coupled with the cathodic reduction of oxygen in the presence of air or water. Unlike many other sulfides such as pyrite, pentlandite and chalcopyrite which are semi-conductors, pyrrhotite is a metallic conductor. The ease with which the different sulfide minerals are prone to oxidation can be determined by a comparison of the rest potentials or open circuit potential, which is the equilibrium potential of the mineral at zero electric current as shown in table 2.4. Understanding the mechanism and factors that affect pyrrhotite oxidation is of importance to interpreting its flotation behaviour, given that the surface species formed on pyrrhotite by the oxidation reaction influences its hydrophobicity and consequent flotation characteristics.

Table 2.4: Rest potential of selected sulfide minerals given as volts versus SHE. From: Kwong *et al.* (2003) and references therein.

Mineral	Formula	Rest Potential (V vs SHE)
Pyrite	FeS_2	0.63
Chalcopyrite	$CuFeS_2$	0.52
Chalcocite	Cu_2S	0.44
Covellite	CuS	0.42
Galena	PbS	0.28
Sphalerite	ZnS	-0.24
Pyrrhotite	$Fe_{(1-x)}S$	-0.28

Rest potential measurements of selected minerals sometimes differ slightly from one publication to the next, not only due to the differences in measurement conditions, but also due to differences in the mineralogy of these minerals. For example, the rest potential of pyrrhotite obtained by Buswell and Nicol (2002) at different points in a Merensky plant varied between 0.20 and 0.29 V. Variations in pyrite rest potential have also been reported. For example, Tao *et al.* (2003) used chronoamperometry measurements on natural pyrite samples to show that the stable potential of pyrite varied according to its derivation. Similarly, Lehner *et al.* (2007) examined the influence of arsenic, cobalt and nickel impurities on the reactivity of synthetically doped pyrite and showed that the composition of pyrite influenced

its reactivity. These differences were ascribed to impurities or surface defects and the effect they may have on changing the nature of the pyrite between an *n-type* semiconductor (donor defects) to a *p-type* semiconductor (acceptor defects). The variation between *n-type* and *p-type* semiconducting behaviour in pyrite may correlate with its metal / sulfur ratio. Since the metal / sulfur ratio and trace element composition of pyrrhotite is variable (e.g. Carpenter and Desborough, 1964; Arnold, 1967), differences in the conducting nature of the different pyrrhotites may be expected. Although Theodossiou (1965) examined the behaviour of pyrrhotite and found a change from *n-type* to *p-type* with increasing temperature for the specimen analysed, little detail is given on the exact mineralogy of the sample used.

2.3.1 Pyrrhotite Oxidation Reactions

One of the additional features about pyrrhotite which gives it a unique character is that it exhibits both oxidative and non-oxidative dissolution (Thomas *et al.*, 2000). Oxidative dissolution which is typical of pyrite is often known as acid producing (Equation I), whereas non-oxidative dissolution which is typical of troilite is acid consuming (Equation II; Thomas *et al.*, 2003).

$$FeS_2 + 8H_2O \rightarrow Fe^{2+} + 2SO_4^{2-} + 16H^+ \quad \text{(I)}$$

$$FeS + 2H^+ \rightarrow Fe^{2+} + H_2S \quad \text{(II)}$$

In the presence of oxidising agents such as oxygen or ferric iron that are likely to be fairly abundant in the flotation system, oxidative dissolution would be favoured (Thomas *et al.*, 2003) and therefore only this reaction will be focussed on. The oxidation of pyrrhotite by oxygen may then proceed as given below (Hamilton and Woods, 1984):

$$FeS_{1.13} \rightarrow Fe^{2+} + 1.13S^0 + 2e^- \quad \text{(III)}$$

$$FeS_{1.13} + 4.52\ H_2O \rightarrow Fe^{2+} + 1.13SO_4^{2-} + 9.04H^+ + 8.78e^- \quad \text{(IV)}$$

Given that ferric iron is likely to be a stable reaction product at alkaline conditions, the reactions can be represented as follows:

$$FeS_{1.13} + 3H_2O \rightarrow Fe(OH)_3 + 1.13S^0 + 3H^+ + 3e^- \quad (V)$$

$$FeS_{1.13} + 7.52\ H_2O \rightarrow Fe(OH)_3 + 1.13SO_4^{2-} + 12.04H^+ + 9.78e^- \quad (VI)$$

Hamilton and Woods (1981) showed that SO_4^{2-} production as shown in equations IV and VI was favoured when the reaction was taken to higher potentials. The sulphoxy species ($S_xO_y^{2-}$) has also been reported as an intermediate of the pyrrhotite oxidation reaction (Steger and Desjardins, 1978; Almeida and Giannetti, 2003).

The oxidation of pyrrhotite may also take place with ferric iron as the oxidant as shown by equation VII (Belzile *et al.*, 2004):

$$Fe_{1-x}S + (8-2x)\ Fe^{3+} + 4H_2O \rightarrow (9-3x)\ Fe^{2+} + SO_4^{2-} + 8H^+ \quad (VII)$$

2.3.2 Mechanism of Pyrrhotite Oxidation

Since the early studies of Steger and Desjardins (1978) and Steger (1982) that determined the identity of the oxidation products of pyrrhotite using chemical extractive methods, much understanding has been gained of the oxidation reaction and change in the surface structure of pyrrhotite using spectroscopy techniques such as AES and XPS (e.g. Buckley and Woods, 1985; Jones *et al.*, 1992; Pratt *et al.*, 1994; Mycroft *et al.*, 1995; Legrand *et al.*, 2005a). This has led to some consensus regarding the nature of the pyrrhotite surface structure upon oxidation. All of the abovementioned authors identified the presence of ferric oxyhydroxides at the surface of pyrrhotite overlying another surface zone depleted in iron that may contain disulfides or polysulfides. Using AES, both Mycroft *et al.* (1995) and Pratt *et al.* (1994) determined the depth profiles for iron and sulfur from which a schematic illustration of the oxidation reaction can be shown as illustrated in figure 2.15. The outermost layer comprised of ferric oxyhydroxides is ~ 5 Å in thickness, underlain by a layer of composition FeS_2 which Jones *et al.* (1992) suggested has a disordered pyrite type structure. This is in turn underlain by a mixture of Fe_2S_3 and Fe_7S_8. The oxidised surface zone of pyrrhotite is only ~ 35 Å in thickness, below which the bulk unreacted pyrrhotite occurs (Pratt *et al.*, 1994; Mycroft *et al.*, 1995).

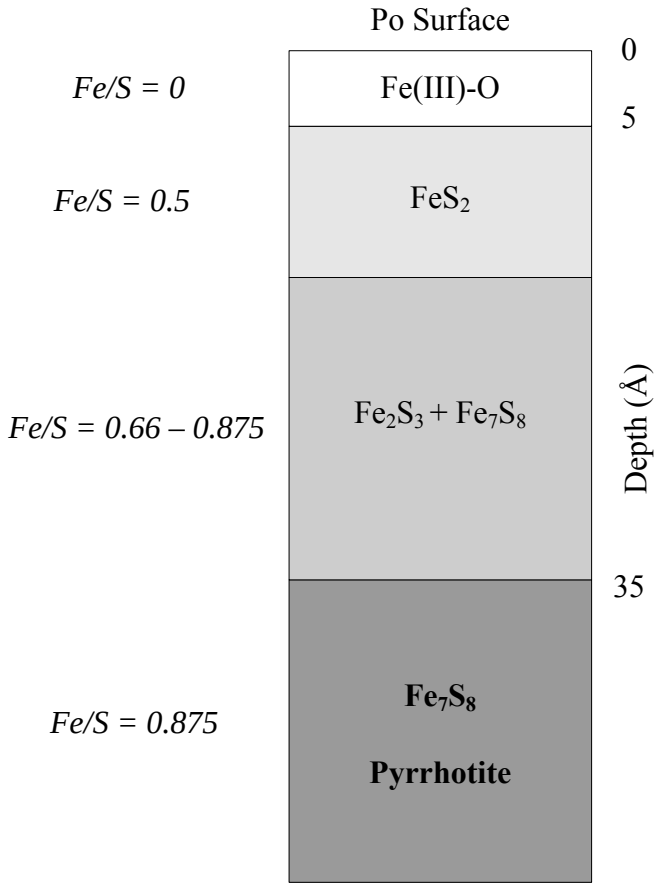

Figure 2.15: Schematic of a cross section through the surface of pyrrhotite during oxidation. Adapted from Mycroft *et al.* (1995).

Based on the species identified with XPS and the AES depth profiling, Pratt *et al.* (1994) proposed the following mechanism for the pyrrhotite oxidation reaction. They suggested that at no time during the oxidation reaction does oxygen significantly diffuse into the sulfide layer and neither does sulfur diffuse to the oxyhydroxide layer. The only movement during the reaction is by the transfer of electrons from the crystal lattice and the diffusion of iron towards the surface ferric oxyhydroxide layer. Pratt *et al.* (1994) proposed that the most reactive sites for oxygen reduction were associated with the ferric iron – sulfur bonds and the vacancies in the pyrrhotite crystal lattice. Vacancies are likely to facilitate electron transfer as well as the diffusion of iron through the lattice resulting in the conversion of the Fe^{3+}-S bonds to Fe^{3+}-O bonds and subsequent ferric oxyhydroxide formation. The formation of the ferric oxyhydroxide layer was observed to decrease over time since it is controlled by the supply of oxygen from the atmosphere, water to the mineral, the rate of diffusion of iron from the underlying sulfur rich layer, and the rate of electron transfer from ferrous iron reduction. The

last two factors are essentially the rate determining steps and may be responsible for the "passivation" of the pyrrhotite surface (Pratt *et al.*, 1994).

Various authors have described the effect of passivation of the pyrrhotite surface by the formation of a layer which prohibits further contact of the pyrrhotite surface with oxygen. This has also been known as an amorphous, non-equilibrium layer which is depleted in iron and may be referred to as the NL layer (Mikhlin *et al.*, 2002). Passivation of the pyrrhotite surface was argued as the mechanism responsible for the decrease in pyrrhotite oxidation at alkaline conditions (Hamilton and Woods, 1981), the interference with collector or activator adsorption mechanisms (Buswell *et al.*, 2002; Gerson and Jasieniak, 2008) and as a potential means of controlling acid mine drainage (Cruz *et al.*, 2005).

In the study of Legrand *et al.* (2005a) that investigated the oxidation reaction of coexisting pentlandite and pyrrhotite, both minerals were observed to form a thin surface layer of ferric oxyhydroxide overlying a metal deficient sublayer. Comparison of the time taken to produce the ferric oxyhydroxide overlayer of similar thickness for pentlandite and pyrrhotite demonstrated that that oxidation reaction was far more rapid for pyrrhotite (5 minutes) relative to pentlandite (30 minutes; Legrand *et al.*, 2005a).

2.3.3 Factors affecting Pyrrhotite Oxidation

Oxygen

Since the oxidation reaction of pyrrhotite is dependent on the presence of oxygen as an oxidising agent, it is expected that a correlation between oxidation rate and the availability of oxygen exists. This correlation was quantified by Lehmann *et al.* (2000) who examined the oxidative dissolution of pyrrhotite by cyanide. Lehmann *et al.* (2000) found that the rate constant of the dissolution reaction showed a progressive increase in magnitude correlating with sparging the solution with nitrogen, air or oxygen. Legrand *et al.* (2005b) similarly examined the influence of the dissolved oxygen concentration on pyrrhotite by investigating the change in the thickness of the ferric oxyhydroxide surface formed during oxidation with XPS. It was shown that as the dissolved oxygen concentration increased, so too did the thickness of the ferric oxyhydroxide surface layer. Spira and Rosenblum (1974) similarly showed an increase in oxygen demand according to whether the pyrrhotite slurry was sparged

with air or pure oxygen. Equation IV is also dependent upon the presence of water and in the early work of Steger (1982), the effect of relative humidity on the oxidation of pyrrhotite was examined. It was shown that the amount of iron and sulfate released by the oxidation reaction positively correlated with an increase in the relative humidity illustrating the dependency of the oxidation reaction on the water or moisture content. Steger (1982) also showed that the oxidised surface changed colour from orange-brown, blue-purple, blue-green back to orange-brown corresponding with the increasing amount of ferric hydroxide produced by the reaction.

Ferric Iron

As shown in equation VII, ferric iron also acts as an oxidising agent for the oxidation of pyrrhotite. Janzen (1996) examined the oxidation of pyrrhotite using ferric iron as the oxidising agent and showed that it followed a Langmuir type adsorption mechanism. The calculated rate constant was approximately ten times greater than that calculated for oxidation by oxygen, suggesting that ferric iron was a much faster oxidising agent than oxygen.

pH

The pH of the solution is known to affect both the nature of the oxidation products produced as well as the rate of the oxidation reaction. Janzen (1996) found an increase in the oxidation rate constant of pyrrhotite corresponding with an increase in pH, suggesting that the oxidation reaction takes place more rapidly in alkaline conditions. Spira and Rosenblum (1974) in their study on pyrrhotite also noted an increase in oxygen demand with increasing pH. Although Chirita *et al.* (2008) investigated the oxidation of troilite and not pyrrhotite, they similarly found an increase in the rate constant of the oxidation reaction when the experiment was performed at a higher pH. In contrast, Hamilton and Woods (1981) showed that the oxidation reaction was retarded at alkaline pH, most likely due to the passivation of the surface layer. The formation of the insoluble ferric hydroxide species is also favoured in alkaline conditions (Hamilton and Woods, 1984).

Temperature

Steger (1982) examined the oxidation of pyrrhotite under a variety of temperatures ranging from 28^0C to 50^0C and showed a corresponding increase in the amount of ferrous iron and sulfate produced with increasing temperature. Based on a model from the Arrhenius equation, Janzen (1996) also found an increase in the oxidation rate of pyrrhotite by 3-5 times for a 20^0

temperature increase with oxygen as the oxidant and an increase by 2-11 times for a 30^0 temperature increase with ferric iron as the oxidant. Similarly, for an increase in temperature from 25 to 40^0C, both the monoclinic and "hexagonal" pyrrhotite examined in the oxidation dissolution study of Lehmann *et al.* (2000) showed a four fold increase in the rate constant.

Crystal Structure

In general, accounts in the literature relating pyrrhotite crystal structure to oxidation or its relative reactivity tend to show little agreement although more frequently suggest that magnetic monoclinic pyrrhotite is the more reactive phase. Janzen (1996) summarised the relevant literature as follows; that Vanyukov and Razumovskaya (1979; In Russian) suggested that the more sulfur rich phase (monoclinic pyrrhotite relative to troilite) had a higher oxidation rate. According to Janzen (1996), Yakhontova *et al.* (1983; In Russian) suggested that the greater amount of vacancies in monoclinic relative to "hexagonal" pyrrhotite allowed for easier electron transfer facilitating the oxidation reaction. In contrast, the study of Orlova *et al.* (1988; In Russian) suggested that "hexagonal" pyrrhotite was more easily oxidised than monoclinic pyrrhotite due to its lower activation energy. In the study of Janzen (1996) itself, no correlation between pyrrhotite crystal structure and oxidation rate was established. The study of Spira and Rosenblum (1974) that investigated the oxygen demand of various pyrrhotite ores, showed an increased oxygen demand for non-magnetic Noranda pyrrhotite relative to magnetic pyrrhotite. However, it was noted by Spira and Rosenblum (1974) that the non-magnetic pyrrhotite sample was probably troilite. More recently, Lehmann *et al.* (2000) determined larger rate constants for the oxidation of monoclinic relative to "hexagonal" pyrrhotite. The associated activation energy for the oxidation reaction was also lower for monoclinic pyrrhotite relative to "hexagonal" pyrrhotite (Lehmann *et al.*, 2000). Comparison of the amount of dissolved and EDTA extractable nickel, iron and sulfur ions from a pyrrhotite mineral slurry by Gerson and Jasieniak (2008) showed that the concentration of these species associated with the oxidation reaction was greater for monoclinic pyrrhotite relative to "hexagonal" pyrrhotite. This suggests that the monoclinic phase underwent more extensive oxidation than "hexagonal" pyrrhotite.

Trace Element Content

Similarly to the role of crystal structure and its effect on pyrrhotite oxidation, the effect of trace metal content on pyrrhotite oxidation is unclear. Kwong (1993) found a semi-quantitative correlation between trace metal content and oxidation rate for monoclinic

pyrrhotite. In his study, samples enriched in nickel and cobalt tended to oxidise slightly slower. When elements to the right of iron on the periodic table (Co, Ni) substitute for iron, they are likely to cause a positive effective charge because of donor defects (Janzen, 1996). The implication of a positive effective charge within the vicinity of nickel substitution sites would be to retard the movement of electrons, thereby inhibiting the oxidation process. In the study of Janzen (1996), no correlation between oxidation rate and trace metal content was found. However, it should be noted that Janzen (1996) compared a variety of pyrrhotite samples from different locations, of which only a quarter of the samples examined were associated with pentlandite which is the focus of this study.

Although the presence of dissolved oxygen in the pyrrhotite structure and its effect on pyrrhotite reactivity have not previously been rigorously evaluated, this does not negate that it may be of importance in influencing pyrrhotite oxidation. Magnetite has been described as an important accessory phase present in some massive sulfide ores (e.g. Sudbury; Naldrett and Kullerud, 1967). This is indicative of the presence of oxygen during the formation and cooling of the MSS. The relationship between iron, sulfur and oxygen during cooling and crystallisation of silicate melts, has in the past been extensively investigated (e.g. Kullerud, 1957; Naldrett, 1969; Shima and Naldrett, 1975). In addition to the relationship between pyrrhotite and magnetite, oxygen can also occur within the pyrrhotite structure. Graham and Mc Kenzie (1987) successfully detected oxygen in the pyrrhotite crystal structure using neutron microprobe techniques to a level of ~ 0.05 wt%. According to Graham *et al.* (1987), the magnetic properties of monoclinic pyrrhotite derived from different sources may be quite variable due to the relative degree of magnetite association, degree of oxidation and also presence of chemical impurities. Therefore the possibility exists, that the presence of oxygen in pyrrhotite may influence its reactivity.

Galvanic Effects

Due to the conductive or semi-conductive nature of the sulfide minerals, they can facilitate electron transfer when they come into contact with one another in a mineral slurry or solution (Ekmekci and Demirel, 1997). Under these circumstances, the mineral with the higher rest potential causes the cathodic reduction of oxygen at the mineral surface, whereas the mineral with the lower rest potential acts as the anode and is oxidised through a reaction such as that illustrated in figure 2.16. According to Rand (1977) the relative rest potentials of the sulfide

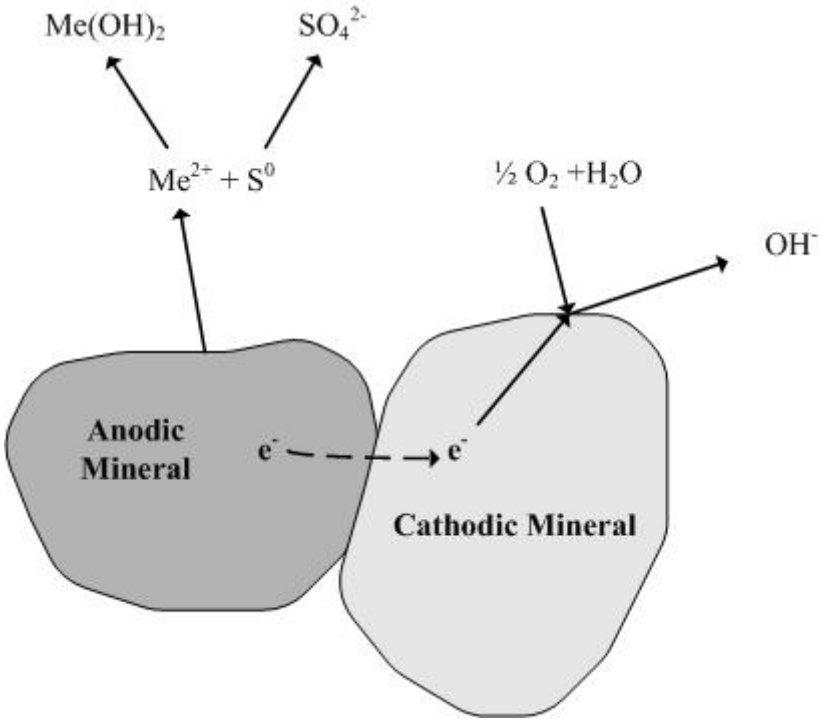

Figure 2.16: Schematic of the galvanic interaction between pyrrhotite (anode) and a more noble sulfide mineral such as pyrite or pentlandite (cathode). Adapted from: Ekmekci (2008).

minerals can be ranked as follows:

Pyrite > Pentlandite > Chalcopyrite > Arsenopyrite > Pyrrhotite > Galena

For pyrrhotite in nickel and platinum group element ore deposits, pentlandite is the more noble mineral with the higher rest potential and likely accelerates the oxidation of pyrrhotite. Pyrite may also occur in this mineral system and would have an even more severe effect on pyrrhotite due to its very noble character. Studies examining the galvanic interaction between pentlandite and pyrrhotite have tended to focus on how this interaction affects the adsorption of flotation reagents and its implications on flotation performance and not on pyrrhotite oxidation (e.g. Bozkurt *et al.*, 1998; Khan and Kelebek, 2004).

2.3.3 Electrochemical measurements of pyrrhotite

Measurement of electrochemical reactions

The measurement of pyrrhotite electrochemical reactions can be divided into two categories, based upon whether the measurement is taken using standard chemical probes (e.g. Dissolved oxygen, pH or ORP) or with the use of a working electrode. Measurements using standard probes are usually taken in mineral slurries or flotation cells, such as the measurement of the ORP or oxygen demand (e.g. Ekmekci et *al.*, 2003). The Magotteaux mill is one such device that not only allows for this type of measurement, but also allows one the ability to control the pulp chemistry (Greet *et al*., 2004). Various authors such as Johnson and Munro (2008), Greet and Brown (2000) and Spira and Rosenblum (1974) have described the importance of quantifying the oxygen demand of different ore types with respect to their flotation performance. In the past, a variety of methodologies have been developed in order to do this, based upon the original method described by Spira and Rosenblum (1974). In general, a freshly ground mineral slurry is purged with air or oxygen and the decay of oxygen with time is measured and quantified (Spira and Rosenblum, 1974; Greet and Brown, 2000; S.H. He *et al.*, 2008). The methodology used to quantify oxygen uptake in this study is based upon that developed by Afrox (Afrox, 2008) and is described in more detail in Section 3.4.

Alternatively, electrochemical reactions can be measured with the use of a working electrode manufactured from pure mineral specimens. Measurements are made by either immersing the working electrode into a buffer solution or into a mineral slurry such as a flotation cell (e.g. Hamilton and Woods, 1981; Buswell and Nicol, 2002) in the presence of counter electrode (e.g. Pt) and a non-polarisable reference electrode (e.g. SHE, SCE or Ag/AgCl). Based on this experimental set up, a number of different electrochemical measurements can be made including rest potential, cyclic voltammetry, chronoamperometry and impedance spectroscopy. Further details of these measurement types can be found in Mendiratta (2000), Buswell and Nicol (2002) and Tao *et al.* (2003).

Measurement of electrochemical reaction products

In order to identify the reaction products on the pyrrhotite surface, a number of different measurements have been used. This includes in-situ XPS analysis where the binding energy of various ionic species (e.g. Fe *2p*) are measured and the peaks assigned to different bond types (e.g. Fe^{2+}-S, Fe^{3+}-S, Fe^{3+}-O). The use of ToF-SIMS allows the distribution of surface

species on particles to be examined with the use of in-situ chemical maps (e.g. distribution of $Fe(OH)^{+}$; Shackleton, 2003; Gerson and Jasieniak, 2008). Alternatively, spectroscopic studies including UV and FTIR techniques have been used to measure the reaction products of pyrrhotite with xanthate collectors (Fornasiero *et al.*, 1995; Bozkurt *et al.*, 1998). Lastly, one of the more popular techniques to measure electrochemical reaction products is EDTA dissolution. It is based on the ability of EDTA to dissolve soluble oxidation products which can be later analysed with standard chemical assay methods (Rumball and Richmond, 1996; Gerson and Jasienek, 2008).

2.4 Pyrrhotite Flotation

2.4.1 Principles of Flotation

Froth flotation is a physico-chemical process that harnesses the difference in surface properties using air bubbles in a flotation cell to separate valuable minerals from the gangue minerals in an ore. The theory of froth flotation has been extensively investigated and reviewed in the past (Sutherland and Wark, 1955; King, 1982; Wills and Napier-Munn, 2006) and so will not be expanded upon here. However, in order to manipulate the nature of the surface species of the valuable mineral (e.g. pyrrhotite with associated PGE and PGM, Merensky Reef) or gangue minerals (e.g. pyrrhotite in Ni ore, Sudbury) a variety of chemical reagents such as collectors, activators, depressants and modifiers are added. In general, the flotation system is affected by numerous parameters (Klimpel, 1984) including equipment (e.g. cell design, air flow), chemical (e.g. collector, activator, pH) and operational components (e.g. mineralogy, feed rate, particle size). In this study of pyrrhotite flotation, the focus is on pyrrhotite mineralogy and how it affects flotation performance. In order to do this, an understanding of the interaction of the pyrrhotite surface with chemical reagents is needed, with specific reference to xanthate collectors and copper activation.

2.4.2 Collectorless flotation of Pyrrhotite

In the past, there have been accounts of the collectorless, natural or self induced flotation of pyrrhotite (e.g. Heyes and Trahar, 1984; Hodgson and Agar, 1984). The mechanism by which this occurs has been heavily debated upon, although Heyes and Trahar (1984) suggested that pyrrhotite self flotation occurs through mild oxidation and the formation of elemental sulfur. Hodgson and Agar (1984) however, suggested that the formation of a stable $Fe(OH)S_2$ intermediate species renders pyrrhotite its hydrophobicity. Others have suggested that the formation of polysulfides and metal deficient sulfides as well as elemental sulfur from pyrrhotite oxidation may provide the necessary hydrophobicity to cause the natural flotation of pyrrhotite (Hamilton and Woods, 1981; Buckley and Woods, 1985; Legrand *et al.*, 2005a). General agreement however, exists that extensive oxidation of pyrrhotite is detrimental to its flotation performance due to the formation of the hydrophilic ferric hydroxide species through a reaction such as that given in equations III-V (e.g. Rao and Finch, 1991; Kelebek, 1993).

Since the solubility of the ferric hydroxide species is considerably lower at a higher pH, so it is observed that the natural floatability of pyrrhotite decreases with increasing pH. Miller *et al.* (2005) have similarly shown a decrease in the contact angle of pyrrhotite with increasing pH illustrating the increase in the hydrophilic character of pyrrhotite to more alkaline conditions.

2.4.3 Flotation with Xanthate Collectors

In most mineral processing operations, chemical reagents are added to enhance the hydrophobicity of the valuable minerals. Although there is a suite of thiol collectors available for use in flotation (Adkins and Pearse, 1992), only the xanthate group is used in this study. Some commonly occurring xanthates including sodium isobutyl xanthate (SIBX) and sodium normal propyl xanthate (SNPX) are illustrated in figure 2.17. The xanthate collectors occur in varying chain lengths, and it well-known that an increase in chain length is associated with a lower solubility product and hence increase in hydrophobicity (M.C. Fuerstenau, 1982). The trade off however, is that an increase in collector chain length is normally associated with a decrease in selectivity (e.g. Mbonambi, 2009).

Collector bonding to the sulfide mineral is generally accepted to be via an electrochemical reaction, where M is the metal, X is xanthate and X_2 is dixanthogen:

$$MS + X^- \rightarrow MX + S + e^- \qquad \text{(VIII)}$$

$$MS + 2X^- \rightarrow MX_2 + S + 2e^- \qquad \text{(IX)}$$

The metal xanthate may in turn be oxidised to the dixanthogen species (Equation IX) depending on the rest potential of the mineral relative to that of the xanthate oxidation reaction. Harris and Finkelstein (1977) showed differences in the rate of oxygen consumption of different chain length collectors due to differences in collector oxidation rate. FTIR and UV spectroscopic studies have suggested that dixanthogen tends to be the more commonly occurring collector species on pyrrhotite under standard oxidising conditions and is the species responsible for rendering pyrrhotite its hydrophobicity during flotation (Allison *et al.*, 1972; Fornasiero *et al.*, 1995; Bozkurt *et al.*, 1998). Fornasiero *et al.* (1995) showed that the

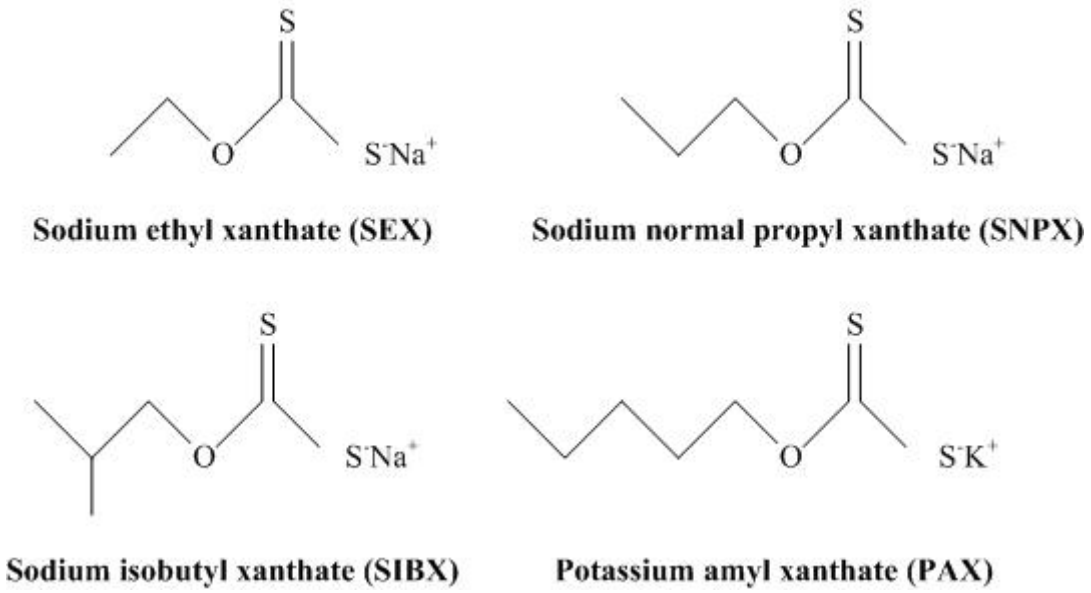

Figure 2.17: Structure of some commonly occurring xanthate collectors used in flotation, including SNPX and SIBX which are used in this study.

xanthate adsorption rate and consequent dixanthogen formation were dependent on pH, and decrease with an increase in pH of the mineral solution. The stability of the xanthate and dixanthogen species is also dependent on solution pH (M.C. Fuerstenau, 1982).

Leppinen (1990) showed some discrepancy when comparing flotation recovery with xanthate adsorption on pyrrhotite throughout the pH range. Even though the maximum xanthate adsorption was at pH 5.5, two peaks in pyrrhotite flotation recovery were observed. The first peak was at pH 3 and then a second minor peak at pH 8 was observed, even though xanthate adsorption was effectively at a minimum at pH 8. The majority of flotation studies however, show that pyrrhotite flotation in the presence of thiol collectors is poor at alkaline conditions and is progressively inhibited as the pH is increased (e.g. Rao and Finch, 1991; Kalahdoozan, 1996; M.F. He *et al.*, 2008). The reason for the reduction in pyrrhotite flotation with increasing pH is described by the Barsky relationship where $[X^-]/[OH^-] = K$ (Kelebek *et al.*, 2007) in that the presence of excess hydroxide anions in solution interferes with xanthate adsorption.

It is known that some degree of oxidation is necessary for both the collectorless and the collector induced flotation of pyrrhotite (Heyes and Trahar, 1984; Kelebek *et al.*, 2007). For collector induced flotation, the presence of oxygen is required for the oxidation of xanthate to

dixanthogen, which is the collector species that renders pyrrhotite its hydrophobicity. The presence of additional minerals to the pyrrhotite system can however, interfere with xanthate adsorption. Bozkurt *et al.* (1998) measured open circuit potentials for both pyrrhotite and pentlandite as single mineral systems and found pentlandite to have a higher potential than pyrrhotite (~100 versus ~ 60 mV SCE, respectively). In the presence of xanthate however, the potentials were reversed and the equilibrium potential of pentlandite was considerably lower than before (-55 mV SCE), whereas for pyrrhotite it was only slightly reduced (40 mV SCE). These results were interpreted by Bozkurt *et al.* (1998) to suggest the establishment of a galvanic interaction, characterised by the anodic oxidation of xanthate on pentlandite and the cathodic reduction of oxygen on pyrrhotite. Consequently, pyrrhotite flotation would suffer due to the enhanced floatability of pentlandite.

S.H. He *et al.* (2008) also considered the effect of a galvanic interaction when trying to account for the differences in pyrrhotite and pentlandite flotation between the scavenger cleaner feed (non-magnetic) and magnetic pyrrhotite concentrate streams treating Sudbury ore at the Clarabelle Mill. One of the mechanisms proposed for the enhanced recovery of pentlandite in the magnetic concentrate stream was the greater abundance of pyrrhotite in the magnetic concentrate stream (59.8 %) relative to the scavenger cleaner feed (25.6 %). If preferential oxidation of pyrrhotite occurred, then oxidation of pentlandite and the consequent reduction in pentlandite floatability would have been prevented.

Pyrite is also more noble than pyrrhotite (Rand, 1977) and it would be anticipated that the preferential oxidation of pyrrhotite and reduction in its floatability would occur relative to pyrite, similarly to the reaction between pentlandite and pyrrhotite as described by S.H. He *et al.* (2008). However, the study of Nakazawa and Iwasaki (1995) showed an enhancement in pyrrhotite flotation recovery when in contact with pyrite.

An additional variable responsible for causing galvanic interactions with pyrrhotite during flotation is that of the grinding media in milling, whether it is mild steel, high chromium steel or ceramic media. In general, steel grinding media have lower rest potentials than pyrrhotite and are oxidised during grinding thus preventing the oxidation of the sulfide minerals themselves. Adam and Iwasaki (1984) observed a reduction in pyrrhotite flotation according to whether the ore was prepared using stainless steel, mild steel, zinc or magnesium grinding media. They suggested that passivation of the pyrrhotite surface occurred by the formation a

ferric hydroxide surface layer due to the disassociation and release of ferrous iron from pyrrhotite. Kirjavinen *et al.* (2002) however, argued that the iron particles adhered to the sulfides were derived from the grinding media. The presence of these particles resulted in poor xanthate adsorption and sulfide flotation but only for the first few minutes of flotation. Once relaxation took place, pentlandite and pyrrhotite experienced some mild oxidation and the floatability was restored. An improvement in pentlandite and pyrrhotite flotation was also observed following grinding in ceramic media relative to steel media (Kirjavinen *et al.*, 2002).

Kirjavinen *et al.* (2002) further investigated the effect of ions derived from the process water on pyrrhotite flotation. The presence of both Ca^{2+} and $S_2O_3^{2-}$ ions served to improve pyrrhotite floatability although not to the same extent as pentlandite. Hodgson and Agar (1989) also investigated the effect of ions in the process water on pyrrhotite flotation and concluded that the presence of Ca^{2+} increased the required dosage of xanthate to cause hydrophobicity due to the competitive adsorption of Ca^{2+} for xanthate with the mineral surface. In the study of Rao and Finch (1991) on xanthate adsorption, it was observed that the presence of Ca^{2+} ions was only beneficial to pyrrhotite recovery at pH 8.4 with nitrogen as the flotation gas. For the other conditions tested (air, pH 6), negligible difference in pyrrhotite recovery was obtained for tests with and without the presence of Ca^{2+} ions. Rao and Finch (1991) suggested that under these conditions (pH 8.4, N_2, 300 ppm Ca^{2+}), the formation of $Ca(OH)^+$ as a surface species would have helped to enhance xanthate adsorption.

The results comparing magnetic and non-magnetic pyrrhotite flotation performance in the presence of xanthate collectors tend to have been quite mixed. According to Iwasaki (1988), it was noted by Harada (1967; In Japanese) that samples of freshly ground monoclinic pyrrhotite were more floatable than “hexagonal” pyrrhotite although the reverse occurred on more oxidised samples. Kalahdoozan (1996) compared the flotation response of synthetic monoclinic, natural monoclinic (magnetic) and synthetic “hexagonal” (non-magnetic) pyrrhotite at a variety of different conditions. The flotation results obtained by Kalahdoozan (1996) were consistent with the results of the adsorption studies. Both sets of results showed synthetic monoclinic pyrrhotite was more floatable at a pH between 7 and 8.5, whereas synthetic “hexagonal” pyrrhotite was more floatable at a pH greater than 10. The natural monoclinic pyrrhotite sample was however, the most floatable for the entire pH range tested. In this study there was no comparison with a natural “hexagonal” pyrrhotite sample, and all

microflotation tests were performed with nitrogen as the flotation gas and may therefore not be entirely representative of the processing of a real ore.

More recently, M.F. He *et al.* (2008) examined the effect of crystallography on pyrrhotite flotation although the focus was on pyrrhotite derived from the Mengzi lead zinc ore in China. Using monoclinic and "hexagonal" pyrrhotite derived from this ore, the flotation performance of pyrrhotite was compared with sodium butyl xanthate, sodium diethyl dithiocarbamate and butyl dithiophosphate. For both pyrrhotite types examined, the maximum flotation recovery was obtained at ~ pH 7. For the pH range tested (4-13), monoclinic pyrrhotite was more floatable than "hexagonal" pyrrhotite.

It does not appear that the role of trace metal content has been investigated with respect to pyrrhotite flotation performance, although Chanturia *et al.* (2004) examined the difference in flotation response of nickel rich, cobalt rich and iron rich pentlandite. Since pyrrhotite and pentlandite are both monosulfides containing similar elements, a comparison can be made. Nickel rich pentlandite exhibited the best flotation performance followed by cobalt rich pentlandite, whereas iron rich pentlandite was the least floatable. Chanturia *et al.* (2004) suggested that differences in the open circuit potential resulting in the preferential formation of hydrophobic elemental sulfur species or preferential xanthate adsorption on the nickel rich pyrrhotite could be responsible for the differences observed in flotation performance.

2.4.4 Activation of Pyrrhotite

In order to improve the efficiency of the adsorption of thiol collectors to sulfide minerals during flotation, an activator is used. Activators typically include metal cations such as copper, lead, silver, cadmium, mercury, nickel and iron, although activation with copper appears to have been the most widely studied and reviewed (D.W. Fuerstenau, 1982; Finkelstein, 1997; Chandra and Gerson, 2009). These studies have tended to focus on the classical activation mechanism, shown here for sphalerite as follows:

$$Cu^{2+} + ZnS \rightarrow CuS + Zn^{2+} \qquad (X)$$

The reaction has been argued to take place by a direct ion exchange mechanism of cupric copper for Zn^{2+} followed by the rapid reduction of cupric copper to cuprous copper and the formation of a hydrophobic CuS or covellite like surface. With the subsequent addition of xanthate collector, a hydrophobic copper-xanthate species is likely to form. Copper activation is heavily influenced by the pH of the solution due to the solubility of the different copper species. At alkaline pH, the copper added to the system may precipitate as a hydrophilic copper hydroxide type species which can potentially react with the collector causing inadvertent activation of gangue minerals (e.g. Nagaraj and Brinen, 1996; Malysiak *et al.*, 2002).

Early studies of the copper activation mechanism for pyrrhotite suggested one similar to sphalerite (Nicol, 1984), although more recently it has been proposed that the copper activation of pyrrhotite is not through direct ion exchange but rather an ion adsorption mechanism similar to that for pyrite (Gerson and Jasieniak, 2008). Using ARXPS, SIMS and chemical analysis, Weisener and Gerson (2000) suggested that pyrite activation occurs through direct adsorption of cupric copper onto the pyrite surface followed by in-situ reduction of cupric copper to cuprous copper. At no point during the reaction do the copper ions migrate into the bulk of the pyrite, but they rather remain as a monolayer on the pyrite surface. Following the reduction of cupric copper, an overlayer of $Cu(OH)_2$ formed when the reaction occurred at alkaline conditions. Similarly, Gerson and Jasieniak (2008), demonstrated an ion adsorption mechanism for pyrrhotite activation. They showed the presence of both cuprous and cupric ions on the pyrrhotite surface and that the Cu^{1+} / Cu^{2+} ratio showed a progressive decrease with increasing oxidation of the pyrrhotite.

Since the majority of mineral processing operations operate within an alkaline pH, the activation of pyrrhotite by copper during flotation at these conditions is of key interest. In the study of Nicol (1984), copper activation only served to improve pyrrhotite flotation recovery at pH 5, whereas at pH 8, there was no improvement in pyrrhotite floatability. Similarly, Miller *et al.* (2005) showed no difference in pyrrhotite contact angle at alkaline conditions with or without copper activation. However, numerous other authors including Leppinen, (1990), Senior *et al.* (1995), Kalahdoozan (1996) and Wiese *et al.* (2007) have shown an improvement in pyrrhotite floatability with copper activation conditions at alkaline pH. Leppinen (1990) showed that the maximum pyrrhotite recovery was obtained at pH 8, even though the accompanying adsorption tests showed very low xanthate adsorption at this pH.

The discrepancy in these results relating to copper activation may be related to the nature of the pyrrhotite sample in terms of its degree of oxidation or crystallography. In the work of Wiese *et al.* (2005) which compared the flotation performance of pyrrhotite from different mines of the Merensky Reef, it was shown that the effect of copper activation was quite different between the ores. For one of the ores, the addition of copper caused relatively little improvement in pyrrhotite recovery whereas for the other ore, there was 50 % improvement in pyrrhotite recovery with copper activation.

In the study of Kalahdoozan (1996) that compared the flotation and adsorption characteristics of monoclinic and "hexagonal" pyrrhotite, all samples examined at pH 10 showed some improvement in floatability with copper activation. At this pH, the natural monoclinic pyrrhotite sample was the most floatable whereas the synthetic monoclinic pyrrhotite sample examined was the most sensitive to changes in collector concentration. More recently, M.F. He *et al.* (2008) examined the flotation response of monoclinic and "hexagonal" pyrrhotites for a variety of thiol collectors at different pH conditions with and without copper activation. Their results showed that the monoclinic pyrrhotite was more sensitive to copper addition than "hexagonal" pyrrhotite.

Although Gerson and Jasieniak (2008) did not evaluate the flotation response of pyrrhotite subsequent to copper activation, their study compared the effect of surface oxidation on both monoclinic and "hexagonal" pyrrhotite at pH 9. The ToF-SIMS analyses in their study showed that with increasing the conditioning time during sample preparation, there was an associated increase in the degree of oxidation on the pyrrhotite surface. Monoclinic pyrrhotite was shown to be more severely oxidised than "hexagonal" pyrrhotite under the conditions studied. It was also shown that oxidation of the mineral surface prior to copper activation could prove to be detrimental for subsequent copper activation. Following the copper activation of pyrrhotite, the mineral surface was stabilised and less likely to be prone to further oxidation.

In addition to copper causing activation of pyrrhotite, Yoon *et al.* (1995) as well as Xu and Wilson (2000) attributed the flotation of pyrrhotite and decrease in pyrrhotite – pentlandite selectivity at the Clarabelle Mill in Sudbury to the inadvertent activation by nickel ions. Yoon *et al.* (1995) detected both nickel and copper ions on the surface of pyrrhotite using LIMS. Xu and Wilson (2000) showed a change in the concentration of nickel ions in the process water

between seasons corresponding to differences in element solubility with temperature change. Increased nickel contents during winter were argued to cause inadvertent flotation of pyrrhotite and the resultant decrease in flotation selectivity.

2.4.5 Pyrrhotite Rejection

In the past there have been numerous strategies which have been investigated in laboratory scale tests for the rejection of pyrrhotite in order to cause selective flotation of pentlandite over pyrrhotite in nickel processing operations (Wells *et al.*, 1997). These strategies include:

(i) Pyrrhotite rejection with magnetic separation
(ii) Pyrrhotite depression with oxygen in flotation
(iii) Pyrrhotite depression with nitrogen in flotation
(iv) Pyrrhotite depression with cyanide in flotation
(v) Pyrrhotite depression with chelating agents in flotation
(vi) Pyrrhotite depression with polymeric depressants in flotation

Although not all of these strategies have been implemented in plant scale processing operations, each of these strategies will in turn be briefly discussed, since some of them will likely influence the flotation behaviour of pyrrhotite.

Pyrrhotite rejection by magnetic separation

One of the first measures that was implemented by the Sudbury nickel processing operations following their policy decision to reject pyrrhotite was the incorporation of a magnetic circuit (Wells *et al.*, 1997). By installing drum magnetic separators, the magnetic monoclinic pyrrhotite could be separated from the bulk ore and then processed separately as illustrated by the flow sheet shown in figure 2.18 of the Clarabelle Mill in Sudbury. The advantage of this mechanism is that it allows the operation to produce both a high sulfur (magnetic pyrrhotite) and low sulfur (silicate mineral) tails which can be disposed of appropriately (Lawson *et al.*, 2005). Within the magnetic separation circuit however, selectivity between pentlandite and pyrrhotite in flotation still needs to be maintained and therefore additional measures for pyrrhotite depression are needed.

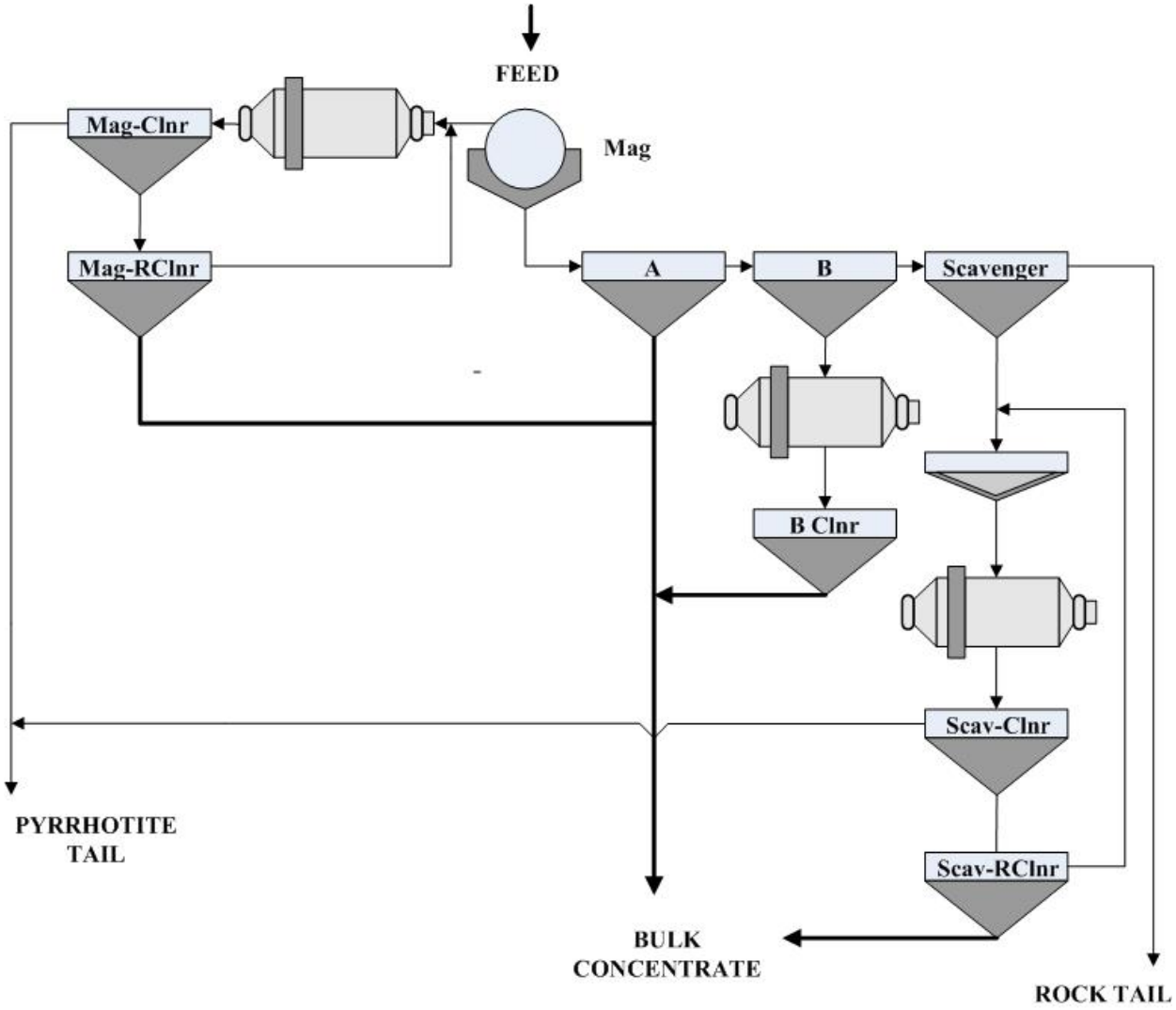

Figure 2.18: Flow sheet of the Clarabelle Mill in Sudbury, Canada, which incorporates both magnetic and non-magnetic circuits, where pyrrhotite rejection is targeted. Adapted from: Lawson *et al*. (2005).

Oxygen depression in flotation

Literature related to the use of oxygen as a pyrrhotite depressant shows contradictory results and this may possibly be resolved by understanding the degree of oxidation. Kelebek (1993) suggested that mild oxidation of pyrrhotite promoted the amount of surface sites available for xanthate adsorption, the production of elemental sulfur and the oxidation of xanthate to dixanthogen. This would account for the good flotation response of pyrrhotite in the stockpiled sulfide ore examined by Kelebek *et al.* (2007). It was suggested that during the stock piling, the pyrrhotite experienced some degree of mild oxidation. However, after extensive oxidation or aeration, the formation of the hydrophilic ferric hydroxides was promoted resulting in the depression of pyrrhotite during flotation. Kelebek (1993) showed a

consistent decrease in pyrrhotite recovery in batch flotation tests with increasing oxidation time of the pyrrhotite prior to flotation.

Nitrogen depression in flotation

The use of nitrogen for potential control during flotation as a means for pyrrhotite depression was investigated by Khan and Kelebek (2004). In the electrochemical study of Khan and Kelebek (2004), a comparison was made of the rest potentials of pyrrhotite and pentlandite with that of the potential for the xanthate to dixanthogen transformation under oxygenated and deoxygenated conditions. On the basis that the formation of dixanthogen was essential for pyrrhotite flotation but not pentlandite flotation, a strategy was proposed. By controlling the potential of the flotation system to avoid the oxidation of xanthate to dixanthogen, the flotation of pyrrhotite would be inhibited and so selective pentlandite flotation was likely (Cheng *et al.*, 1994; Khan and Kelebek, 2004).

Cyanide depression in flotation

Kalahdoozan (1996) investigated the use of sodium cyanide as a pyrrhotite depressant at alkaline pH. The exact mechanism by which cyanide causes pyrrhotite depression is unclear, although numerous suggestions including the formation of metal cyanide complexes and the decomposition of adsorbed dixanthogen have been proposed (Prestidge *et al.*, 1993). Although the use of cyanide as a depressant showed promise in laboratory scale test work (Kalahdoozan, 1996), it has not been implemented on industrial processing operations due to the associated environmental concerns with the handling and treatment of this hazardous chemical (Wells *et al.*, 1997).

Depression with amines

The current methodology used for pyrrhotite depression in the Sudbury ores is with the use of the chelating agents, DETA or TETA in conjunction with sodium metabisulfite (Lawson *et al.*, 2005). Kelebek and Tukel (1999) showed that use of TETA alone or use of sodium metabisulfite by itself showed little depressing effect on pyrrhotite, but when the two reagents were used in conjunction with one another, effective pyrrhotite depression was achieved. LIMS analysis in the study of Yoon *et al.* (1995), showed both nickel and copper ions on the pyrrhotite surface in the flotation concentrate that were most likely derived from the process water and which inadvertently activated the pyrrhotite. It has been argued that both DETA and TETA are able to form stable complexes or chelates with these heavy metal ions that

prevent the inadvertent activation of pyrrhotite (Kelebek *et al.*, 2005). The addition of sulfite in conjunction with TETA has been proposed to assist in maintaining low redox potentials and thereby inhibit the formation of hydrophobic sulfur species (Kelebek *et al.*, 2005).

Depression with polymeric depressants in flotation

For some of the platinum deposits in South Africa, there is no association of pyrrhotite with the platinum group minerals and only the pentlandite and chalcopyrite are of interest. In the flotation of these ores, polymeric depressants are used to reduce the floatable silicate gangue minerals such as talc (Wiese *et al.*, 2005). In order to investigate whether these same polymeric depressants could perform an additional role in promoting the selective flotation of pentlandite, Mbonambi (2009) conducted microflotation tests on pentlandite and pyrrhotite. Mbonambi (2009) showed that the combination of a guar depressant with SNPX at high pH could cause some depression of pyrrhotite for selective pentlandite flotation.

2.4.6 Comparison of plant operating strategies for pyrrhotite flotation and rejection

In flotation operations where pyrrhotite recovery is targeted for its association with the platinum group minerals and elements, pyrrhotite is recovered through a bulk sulfide float (e.g. Merensky Reef). These operations generally use an MF2 (mill-float, mill-float) circuit configuration comprising fine grinding in the regrind stage to optimise the liberation of the fine grained platinum group minerals. Thiol collectors are normally used to recover the sulfides chalcopyrite, pentlandite and pyrrhotite. Copper sulfate is used as an activator to enhance the recovery of the slower floating pyrrhotite in some operations (Miller *et al.*, 2005; Vos, 2006). Polymeric depressants such as carboxymethylcellulose (CMC) or guar gum are also used to depress the naturally floating gangue minerals present in the ore and bulk flotation occurs at the natural pH of the ore, which is ~ 9 (Wiese *et al.*, 2005).

Following the move in the early 1980's to target pyrrhotite rejection due to high sulfur dioxide emissions in the smelters treating Sudbury ores and its detrimental effect on the environment, these operations have had to implement numerous steps to optimise pyrrhotite rejection while still maintaining selectivity between pyrrhotite and pentlandite (Pietrobon and Grano, 2001). These Sudbury operations now use two circuits as illustrated in figure 2.18; a magnetic circuit for treating magnetic monoclinic pyrrhotite and non-magnetic circuit for

treating "hexagonal" pyrrhotite, pentlandite and chalcopyrite (Wells *et al.*, 1997; Lawson *et al.*, 2005). In order to maintain selectivity between pentlandite and pyrrhotite during flotation numerous reagent schemes have been tried and tested on these plants including the use of cyanide, nitrogen and oxygen (Wells *et al.*, 1997). The preferred reagent scheme which is currently used on these operations as pyrrhotite depressants are the amines DETA or TETA in conjunction with sodium sulfite (Lawson *et al.*, 2005). Flotation normally occurs around pH 9.2 for the Sudbury ore and progressively drops through the circuit down to ~ 8 (Kelebek *et al*., 2007). At Nkomati Nickel in South Africa, a proprietary depressant comprised of a modified polyacrylamide blend of sulfite and sulfate is used as their preferred pyrrhotite depressant.

2.5 Process Mineralogy

Process Mineralogy, a subdivision of the field of geometallurgy (Hoal, 2008; Walters, 2008), is the application of mineralogy to the mineral processing industry (Petruk, 2000). The earliest accounts of process mineralogy in practice extend back to Irving (1906), Gaudin (1939) and Stillwell and Edwards (1945). Consequently, it has been reviewed several times in the past e.g. Petruk (2000), Baum *et al*. (2006). Due to the comprehensive nature of the account of Henley (1983), this review will be focussed upon here. Henley (1983) described how mineralogy can be applied right through the fields of exploration and drilling, preliminary metallurgical testing, pilot plant testing, plant design and engineering, plant construction and commissioning as well as during plant operation. The ultimate goal is to develop a predictive model of mineral processing performance from the understanding of the variation of the mineralogy through the flow sheet. In order to achieve this goal, scientific knowledge and techniques are drawn from a number of disciplines including geology, mineralogy, mathematics, sampling statistics, physics, chemistry and engineering (Henley, 1983; Lotter *et al.*, 2002).

Henley (1983) illustrated the need for information on the identity of the minerals present in the ore sample, relative proportions of each phase, mineral composition, liberation characteristics of both valuable and gangue minerals as well as element deportment for the feed, concentrates and tail samples. A variety of analytical methods for determining mineral abundances (grain counting, point counting, gross counting, area counting, image analysis), mineral composition (optical methods, XRD, EMP and proportional dissolution) and mineral liberation (point counting, area counting, image analysis, density separation, and selective dissolution) were reviewed. More recently, the development of key analytical instruments such as QXRD with Rietveld refinement, x-ray computed tomography (X-ray CT), as well as the automated SEM instrumentation, QEMSCAN and MLA have to some degree, made the acquisition of mineralogical data considerably faster, more detailed and statistically representative (Raudsepp *et al.*, 2002; Gu, 2003; Fandrich *et al.*, 2007; Gottlieb, 2008). The focus of much of the literature on process mineralogy has been on the application of these techniques to mineral processing in the form of case studies, as well as use of this information to enhance the models that describe the breakage, liberation and separation processes (e.g. Wightman *et al.*, 2008). Several case studies on process mineralogy are reviewed below.

Several QEMSCAN based case studies have been published by Lotter and his co-workers such as Lotter *et al.* (2002), Baum *et al.* (2006) and Charland *et al.* (2006). The case study of Charland *et al.* (2006) however, is a key example that shows the integration of process mineralogy from plant design to commissioning for the Montcalm nickel copper concentrator in Ontario, Canada. During the prefeasibility and feasibility studies of the Montcalm ore, several geometallurgical end-members were defined by examination of drill core samples based on ore geology, microscopy and QEMSCAN analysis. Disseminated, net-textured and massive sulfide textures were defined as geometallurgical end members and the grinding and flotation characteristics of each of these end members determined. The recognition of potential problematic minerals; presence of pyrite in very variable amounts (effect on pH during flotation), presence of both granular and flame pentlandite (flame pentlandite likely to remain locked unless ultra fine grinding was used) as well as fine grained disseminated chalcopyrite were noted. These mineralogical factors were in turn taken into consideration during plant design. Subsequent bench mark surveys following plant start up were also described and the nature of the losses of locked pentlandite and chalcopyrite to the tails were evaluated by QEMSCAN. Based on the plant survey, it was recommended that some optimisation of the primary grinding circuit was needed to reduce the proportion of fines, a regrind stage was needed to liberate locked chalcopyrite and pentlandite, and further electrochemical control of the pulp chemistry was needed to optimise the rejection of pyrrhotite.

Bojcevski *et al.* (1998) similarly determined the metallurgical performance of different textural types of ore, but the study was focused on the division of the George Fisher lead zinc ore in Australia into a variety of meso and microtextures. The mesotextures identified varied between massive galena, massive sphalerite and galena, massive sphalerite, massive pyrite, banded galena and sphalerite, banded sphalerite and banded pyrite. The metallurgical characteristics in terms of ore feed grade, grindability, proportion of naturally floating material, mineral liberation and flotation were in turn assessed. Based on this information and that gained from the ore microtextures, textural modelling could be conducted so that the performance of any combination of ore types could be predicted. The benefits gained by such an approach during feasibility and production stages were in turn noted by Bojcevski *et al.* (1998). Bojcevski *et al.* (1998) also highlighted the need for interaction between geologists, mining engineers and metallurgists in order to improve overall operating performance.

On similar principles, Johnson and Munro (2008) presented guidelines on how to assign different domains of an ore body based on their metallurgical performance. Physical and chemical properties of the ore which needed to be taken into consideration included the identity of the valuable and gangue minerals, mineral grain size, associations and degree of liberation, and the flotation response as determined by a variety of tests. The oxygen demand, as well as the degree of oxidation of the slurry after grinding were noted as important parameters that also needed consideration, especially if the ore contained significant proportions of pyrrhotite or pyrite.

Process mineralogy has been of particular use to the platinum industry due to the large variation in mineralogy, very low grade of the ores and the ease with which the automated SEM instrumentation (QEMSCAN, MLA) are able to locate the platinum group minerals based on their BSE intensity (Brown and Dinham, 2006; Fandrich *et al.*, 2007). Schouwstra *et al.* (2000) also showed the large variation in mineralogy in terms of the different proportion of platinum group alloys, arsenides, sulfides, tellurides present from one Merensky Reef mine to another. Similarly, the association of these platinum group minerals with the base metal sulfides, silicates and chromite was quite variable. Based on this specific type of information, improved understanding of the grinding, liberation and flotation response of these different platinum group minerals could be employed in order to optimise metallurgical performance (Schouwstra *et al.*, 2000; Nel *et al.*, 2005; Shackleton *et al.*, 2007). Although not focused on the platinum group minerals but rather on the base metal sulfides, Brough (2008) characterised the mineralogy of the Normal, Pothole (P2) and Transitional (NP2) Merensky Reef types. The influence of the geology and mineralogy (base metal sulfide grain size, mode of occurrence, liberation, association etc) on the metallurgical performance of the different ore types was shown. Brough (2008) showed that the plagioclase rich NP2 reef type had the best metallurgical performance in terms of potential mill throughput, base metal sulfide liberation, recovery and amount of floatable gangue.

Nel *et al.* (2005) also used process mineralogy in evaluating the effects of regrind circuit configuration, but with the focus on the expansion project of the UG2 circuit at the Impala Concentrator. Since lower platinum group mineral recovery was achieved than targeted, the project was carried out to examine the effect of a change from a closed to open circuit configuration. It was subsequently shown with the use of QEMSCAN that the change in regrind circuit configuration improved the liberation of the platinum group minerals in the

regrind product. Becker *et al.* (2008) also investigated platinum group mineral liberation in the UG2 ore, but with the focus on quantifying the influence of classification with the 3 product cyclone. It was demonstrated that the 3 product cyclone provided a more efficient means of classification of the dual density UG2 ore than conventional cyclones based on the composition and degree of liberation of the flotation feed as determined by MLA.

2.6 Critical Review of the Literature

2.6.1 Pyrrhotite Mineralogy

Although a significant body of research that was developed over the last 40 years has positively contributed towards the general understanding of the details of pyrrhotite mineralogy (e.g. Nakazawa and Morimoto, 1971; Francis and Craig, 1976; Kissin and Scott, 1982; Powell *et al.*, 2004; Fleet, 2006), the majority of the research has focused on the use of synthetic samples in order to understand pyrrhotite phase relations and determine pyrrhotite crystal structures. Synthetic samples were not only used for experimental phase relation studies due to the nature of the experiments, but also due to the lack of suitable natural pyrrhotite single crystals for structure determination. Similarly, although the compositional variation and nature of the mineral association between natural pyrrhotite samples from a variety of deposits have been examined in the past (e.g. Carpenter and Desborough, 1964; Arnold, 1967), this was based on the d-spacing method of Arnold and Reichen (1962) and not by direct measurement of the composition. In addition, little research has focused on understanding the compositional variation of pyrrhotite within any single ore deposit. Therefore, the application of the fundamental understanding and use of compositional and crystallographic information based on synthetic pyrrhotite are of limited relevance to process mineralogy where natural ores are focused upon.

2.6.2 Pyrrhotite Reactivity

There appears to be a good understanding of the electrochemistry of pyrrhotite in terms of oxidation reactions and the mechanism of oxidation based on the work of Rand (1977), Hamilton and Woods (1981), Pratt *et al.* (1994) and Mycroft *et al.* (1995) to name but a few researchers. However, the accounts with respect to the role of crystallography and trace element content on pyrrhotite oxidation are in conflict (e.g. Kwong, 1993; Janzen, 1996; Gerson and Jasieniak, 2008). Similarly, the presence of ferric iron in the pyrrhotite structure is debatable (Pratt *et al.*, 1994; Mikhlin and Tomashevich, 2005; Letard *et al.*, 2007), even though it may act as an oxidising agent during pyrrhotite oxidation and be a factor responsible for the variation in oxidation rates between pyrrhotite types. In general, little attention was paid to the mineralogy of the pyrrhotite samples upon which the experimental work was

performed and therefore comparison of the results from different studies is difficult. Studies comparing oxidation rates of magnetic and non-magnetic pyrrhotite have used pyrrhotite samples derived from many different localities (e.g. pyrrhotite from nickel copper ore deposits, lead zinc ore deposits or even synthetic pyrrhotite) without consideration that the provenance of pyrrhotite may influence its oxidation.

2.6.3 Pyrrhotite Flotation

A similar situation to pyrrhotite reactivity occurs with respect to the understanding of pyrrhotite flotation; a reasonable understanding exists with regard to the mechanism and species which lend pyrrhotite its floatability (e.g. Allison *et al.*, 1972; Heyes and Trahar, 1984; Hodgson and Agar, 1984; Buckley and Woods, 1985; Fornasiero *et al.*, 1995; Bozkurt *et al.*, 1998), but the accounts comparing the floatability of the different pyrrhotite types are in conflict (e.g. Kalahdoozan, 1996; M.F. He *et al.*, 2008). Since little attention was generally paid to the mineralogy of the pyrrhotite samples used in flotation tests, a comparison of the results from these different accounts is not easy. In addition, experimental work from these literature accounts was based on pyrrhotite samples derived from natural nickel copper ores, lead zinc ores and on synthetic pyrrhotite. The role of mineral chemistry (including trace metal substitution) and mineral association and its effect on flotation performance were not considered in these studies.

2.6.4 Approach of this Thesis

Sections 2.6.1 to 2.6.3 have shown the limitations in the existing literature on pyrrhotite mineralogy, reactivity and flotation performance whereas Section 2.5 has shown the value which process mineralogy can add to mineral processing based on a through understanding of the variation of the mineralogy of an ore. On this basis, a platform is set for the contribution of this piece of research on pyrrhotite flotation that aims to develop the relationship between pyrrhotite mineralogy and flotation performance.

A thorough characterisation of the mineralogy of pyrrhotite from natural nickel and platinum group element ore deposits will contribute to the fundamental understanding of pyrrhotite

mineralogy. The characterisation of natural pyrrhotite using modern analysis methods (e.g. EMP, QXRD, Automated SEM) will also be a notable advance for process mineralogy.

A suitably designed experimental program to explore pyrrhotite reactivity and flotation based on a set of naturally occurring pyrrhotite samples for which the mineralogy has been thoroughly characterised, will provide a unique data set with which to develop the relationship between pyrrhotite mineralogy and flotation. By focussing on naturally occurring pyrrhotite from a single type of ore deposit, additional mineralogical variables associated with ore deposit type that could create further confusion are constrained. Therefore, experimental information on pyrrhotite reactivity and flotation will be of the nature that is amenable to allow only the key mineralogical factors that influence pyrrhotite flotation to be identified.

By using an integrated approach towards the interpretation of pyrrhotite reactivity and flotation performance, an understanding of the mineralogical factors which affect pyrrhotite flotation performance will be gained. Based on this critical review of the literature, the key questions from Chapter 1 are presented again:

(i) Hoes does the mineral association, mineral chemistry and crystallography vary between magnetic and non-magnetic pyrrhotite?

(ii) How does ore deposit formation affect the mineralogy of pyrrhotite?

(iii) How does the reactivity of magnetic and non-magnetic pyrrhotite differ? Can these differences be accounted for in terms of the:
a) crystallography
b) mineral chemistry
c) mineral association of pyrrhotite?

(iv) How does the flotation performance of magnetic and non-magnetic pyrrhotite differ? Can these differences be accounted for in terms of the:
a) crystallography
b) mineral chemistry
c) mineral association of pyrrhotite?